TU Delft

Delft University of Technology

A high-deck coach evacuation model framework
Behavioural modelling, numerical analyses and insights

Huang, Rong; Zhao, Xuan; Yang, Yuzhou; Liu, Qingshan; Yuan, Yufei; Daamen, Winnie

DOI
10.1016/j.ress.2025.111582

Publication date
2025

Document Version
Final published version

Published in
Reliability Engineering and System Safety

Citation (APA)
Huang, R., Zhao, X., Yang, Y., Liu, Q., Yuan, Y., & Daamen, W. (2025). A high-deck coach evacuation model framework: Behavioural modelling, numerical analyses and insights. *Reliability Engineering and System Safety*, *265*, Article 111582. https://doi.org/10.1016/j.ress.2025.111582

Important note
To cite this publication, please use the final published version (if applicable).
Please check the document version above.

Copyright
Other than for strictly personal use, it is not permitted to download, forward or distribute the text or part of it, without the consent of the author(s) and/or copyright holder(s), unless the work is under an open content license such as Creative Commons.

Takedown policy
Please contact us and provide details if you believe this document breaches copyrights.
We will remove access to the work immediately and investigate your claim.

This work is downloaded from Delft University of Technology.
For technical reasons the number of authors shown on this cover page is limited to a maximum of 10.

Green Open Access added to TU Delft Institutional Repository
as part of the Taverne amendment.

More information about this copyright law amendment
can be found at https://www.openaccess.nl.

Otherwise as indicated in the copyright section:
the publisher is the copyright holder of this work and the
author uses the Dutch legislation to make this work public.

Reliability Engineering and System Safety 265 (2026) 111582

Contents lists available at ScienceDirect

Reliability Engineering and System Safety

journal homepage: www.elsevier.com/locate/ress

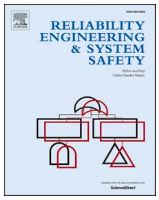

A high-deck coach evacuation model framework: Behavioural modelling, numerical analyses and insights

Rong Huang [a], Xuan Zhao [a,*], Yuzhou Yang [a,*], Qingshan Liu [a], Yufei Yuan [b,*], Winnie Daamen [b]

[a] School of Automobile, Chang'an University, Xi'an 710064, China
[b] Department of Transport and Planning, Delft University of Technology, Stevinweg 1, 2628 CN, Delft, the Netherlands

ARTICLE INFO

Keywords:
High-deck coach
Evacuation model
Strategic behaviour
Tactical behaviour
Operational behaviour
Overtaking behaviour

ABSTRACT

Evacuation from transportation tools is receiving increasing attention due to its high risk and complexity. However, as a crucial travel mode, high-deck coaches, have been overlooked, lacking a dedicated evacuation model, let alone exploratory simulation analyses. This work proposes an innovative high-deck coach evacuation model framework, where three intertwined modules are developed to separately delineate the strategic, tactical and operational passenger evacuation behaviours. In the strategic behaviour module, the Cox-Weibull hazard duration model is introduced to capture the pre-evacuation times of passengers so that both the distribution characteristics and the dependence on the proximity to the target exit are encapsulated. In the tactical and operational behaviour modules, elaborate behavioural rules are designed and coupled with Cumulative Prospect Theory to comprehensively incorporate the typical behavioural characteristics and decision-making factors of passengers. The framework is validated with empirical data from various scenarios and proven to significantly outperform the state-of-the-art passenger evacuation model. It is found that the CWM substantially improves the prediction accuracy of the framework compared with the Weibull probabilistic distribution. Overtaking behaviour significantly affects passenger evacuations, but does not induce any benefit for the overall system. This study offers valuable tools and insights for high-deck coach evacuation simulation and management.

1. Introduction

As one of the major modes of mass transportation, high-deck coaches bring significant convenience to the travel of the public, however, serious accidents occasionally occur, with sometimes catastrophic consequences [1]. Timely evacuation from the coach carriage before the survival condition becomes untenable is essential to reduce or avoid casualties of passengers in case of emergencies [2–4]. High-deck coach evacuation possesses unique characteristics (e.g., extremely confined space, and complicated behaviour of passengers), which are distinct from evacuation from other facilities/modes (i.e., buildings and other transport vehicles) [5,6]. Thus, a dedicated high-deck coach evacuation model that incorporates these environmental and behavioural characteristics is crucial to accurately predict passenger evacuation behaviour, which is essential to assess and improve the evacuation performance of high-deck coaches and to develop evacuation and design guidelines.

However, to our best knowledge, such a model is absent in literature yet [7]. In contrast, there are well-validated models dedicated for other evacuation contexts, including buildings [8], aircraft [9], trains [10], ships [11] and transit buses [12]. These models are generally developed by incorporating context-dependent behavioural rules into a general model (e.g., the cellular automaton (CA) model). This phenomenon emphasises that it is usually hard for an evacuation model to accurately simulate the evacuation from facilities with the configuration and occupant behaviour characteristics that are not considered during modelling. Indeed, previous studies evidenced that for the general models, proper improvements should be made to achieve satisfactory evacuation simulation accuracy for those geometries with dense seat row arrangements [13]. Haghani and Sarvi [14] also suggested that evacuation simulation models should achieve a sufficiently accurate representation of behaviours at the strategic, tactical and operational levels to ensure prediction accuracy. As such, developing a dedicated evacuation model for a specific new scenario has long been recognised as one of the critical challenges in the evacuation safety community

* Corresponding authors.
E-mail addresses: zhaoxuan@chd.edu.cn (X. Zhao), yangyuzhou@chd.edu.cn (Y. Yang), Y.Yuan@tudelft.nl (Y. Yuan).

https://doi.org/10.1016/j.ress.2025.111582
Received 15 March 2025; Received in revised form 18 July 2025; Accepted 12 August 2025
Available online 13 August 2025
0951-8320/© 2025 Elsevier Ltd. All rights are reserved, including those for text and data mining, AI training, and similar technologies.

[15–19]. High-deck coaches, as one kind of common transportation mode, however, belong to new evacuation scenarios that have not been thoroughly studied yet [1,7]. Therefore, the development of a dedicated high-deck coach evacuation model that is validated with empirical data is of particular urgency given its essential role in passenger safety research.

Due to the complexity of the strategic-level behaviour, the induced time delay (i.e., pre-evacuation time) is utilised to reflect its influence on evacuation [20]. In the existing studies of pre-evacuation time modelling, the stochastic approach based on probabilistic distributions dominates, which only considers the distribution characteristics of pre-evacuation times, and thus cannot capture the effect of any influential factors. Nonetheless, numerous empirical observations in different scenarios (e.g., rooms [21], theatres [22] and high-deck coaches [1]) have demonstrated that the pre-evacuation times of occupants not only exhibit specific distribution characteristics but also show a strong dependence on the proximity to the target exit. To resolve this issue, Haghani, et al. [20] proposed to use the Cox proportional hazard duration model. Compared with this method, the stochastic approach based on probabilistic distributions is more straightforward in terms of parameter calibration and generates an input that is widely supported by the existing models. Thus, the question arises as to which approach facilitates higher accuracy of the evacuation simulation outputs from the perspective of the overall performance of the simulation system.

Overtaking behaviour, as one type of operational behaviour, is common in evacuations [23]. Numerous researches have been conducted to capture this behaviour and investigate its potential effects, which mainly focused on unidirectional flow scenarios [24–26] and have begun to make a few attempts to explore more complex scenarios such as aircraft [27] recently. Song, et al. [23] advocated the need to revisit the existing overtaking behaviour modelling methods in confined spaces (e.g., high-deck coaches) due to the distinct behavioural characteristics induced by space limitation. More importantly, existing simulation studies have not shown a complete consensus on the effects of overtaking behaviour yet. Fu, et al. [24] suggested that the overtaking ratio has an invariably positive effect on the unidirectional pedestrian flow, whereas some studies observed the two-sided effects of overtaking behaviour on evacuation efficiency [23,25]. Thus, how to effectively delineate passenger overtaking behaviour in high-deck coaches - typical new scenarios with confined spaces, and its effects on high-deck coach evacuations are still open problems.

In recent years, microscopic evacuation simulation models are receiving increasing attention. Various types of such models have been developed, e.g., force-based models [28], agent-based models [29], and rule-based models [30], among which CA models, as an important branch of rule-based models, have been widely used for different applications owing to various merits [30–32]. Specifically, through approximately adjusting the space discretisation degree and flexibly incorporating various sorts of behavioural rules, CA models are capable of accurately delineating the geometric structure and occupant behaviour characteristics in different facilities, including those with cramped spaces [8,23,33]. Therefore, the CA model would be an eligible general model for developing a dedicated high-deck coach evacuation model and thus used in this paper.

To bridge the gaps mentioned heretofore, this paper proposes an innovative high-deck coach evacuation model framework where the strategic, tactical and operational behaviour modules are developed and intertwined with each other. Secondly, we for the first time calibrate the Cox proportional hazard duration model by empirical data and delve into the efficacy of two widely used pre-evacuation time modelling methods. The third contribution is the systematic investigation on the effects of overtaking behaviour on high-deck coach evacuation efficiency and crowdedness. The proposed model framework is validated and compared to the state-of-the-art commercial evacuation simulation software by using empirical data from various scenarios, which proves its universality and superiority.

The remainder of this paper is structured as follows. Section 2 reviews related works devoted to passenger evacuation modelling of typical public transportation tools. In Section 3, the proposed framework is presented in detail, followed by the simulation setups for the validation, the comparative analyses between two pre-evacuation time modelling methods and the investigation on the effects of overtaking behaviour in Section 4. Section 5 validates the proposed framework with empirical data and presents the simulation results and discussion. Finally, in Section 6, a summary of the main findings and recommendations concludes the paper.

2. Related work

Table 1 summarises existing typical studies of passenger evacuation modelling according to the type of transportation tool, where the used model, the capability of delineating the strategic, tactical and operational (including locomotion movement and overtaking) behaviours, as well as the implementation of the validation procedure are provided detailedly. Also, the evaluation results of the proposed framework are presented in bold in Table 1. This way, the novelty of the proposed framework can be comprehensively and straightforwardly identified.

2.1. Passenger evacuation modelling

Due to the high risk and complexity of evacuation from transportation tools, numerous studies have been devoted to passenger behaviour modelling and simulation of buses [12,35,36], trains [10,37,38], aircraft [9,29,40] and ships [11,42,43], shown in Table 1. However, another common and crucial travel mode, high-deck coaches, has been overlooked, lacking a dedicated evacuation model, let alone exploratory simulation analyses.

The strategic, tactical and operational (locomotion movement and overtaking) behaviours are common in passenger evacuations [14,23]. Accordingly, an eligible passenger evacuation model should be able to reproduce these behaviours, whereas none of the existing models has been demonstrated to possess such a capability (shown in Table 1). Moreover, nearly half of the passenger evacuation models have not been examined by the validation procedure using empirical data, leading to the lack of knowledge on the degree of match between simulations and real situations, let alone tuning the parameters and components to fit another new scenario. On the other hand, more cramped interior layouts and unique evacuation procedures of high-deck coaches result in distinct environment and passenger behaviour characteristics [7]. At the strategic level, empirical observations indicated that the pre-evacuation times of high-deck coach passengers exhibit a strong dependence on the proximity to the target exit [1], yet it has not been embodied in the strategic behaviour module of the existing passenger evacuation models. As for the tactical and locomotion movement behaviour modelling in these models, their risk and uncertainty attributes have been greatly overlooked, while recent studies evidenced the related decision-making characteristics and suggested deploying a descriptive theory, Cumulative Prospect Theory (CPT), to effectively capture them [8]. Thus, it is believed that the existing passenger evacuation models, even the simulation software (e.g., Pathfinder), could not well reproduce passenger evacuation behaviour from high-deck coaches, as demonstrated by our results.

2.2. Pre-evacuation behaviour modelling

Pre-evacuation behaviour modelling is significant for accurate evacuation simulation. Nonetheless, as indicated by Haghani, et al. [20], it has attracted far less attention than tactical and operational level behaviour modelling. To our best knowledge, in most of the evacuation models including the simulation software, the used pre-evacuation time values are obtained by the deterministic user assignment or the stochastic approach based on probabilistic distributions, e.g., [9,10,37,

Table 1
Summary of the existing passenger evacuation modelling studies.

Type of tool	Reference	Model	Strategic behaviour	Tactical behaviour	Operational behaviour		Validation
					Locomotion movement	Overtaking behaviour	
Bus	Lv, et al. [34]	Pathfinder	√	√	√	?	×
	Liang, et al. [35]	STEPS	√	√	√	?	√
	Li, et al. [12]	Force-driven model	×	×	√	×	√
	Xu and Guo [36]	CA model	×	×	√	×	√
Train	Galea, et al. [37]	railEXODUS	√	√	√	?	√
	Qiu and Fang [38]	Legion	√	√	√	?	√
	Huang [13]	Social force model	×	×	√	×	√
	Huang [13]	Agent-based model	×	×	√	×	√
	Najmanová, et al. [39]	Pathfinder	√	√	√	?	√
Aircraft	Galea, et al. [9]	airEXODUS	√	√	√	?	√
	Hedo and Martinez-Val [29]	Agent-based model	√	√	√	×	√
	Liu, et al. [40]	Network model	√	√	√	×	√
	Song, et al. [23]	CA model	×	×	√	√	×
	Melis, et al. [41]	Pathfinder	√	√	√	?	×
Ship	Galea, et al. [11]	maritimeEXODUS	√	√	√	?	√
	Wang, et al. [42]	Eavc	√	√	√	?	×
	Xie, et al. [43]	AnyLogic	√	√	√	?	×
	Xie, et al. [44]	Pathfinder	√	√	√	?	×
	Fang, et al. [45]	Social force model	×	×	√	×	√
	Chen, et al. [46]	CA model	×	√	√	×	×
High-deck coach	**This paper**	**CA model**	√	√	√	√	√

The symbols identify whether the assessed simulation model implements a specific capability/procedure (√=yes, ×=no, and ?=unproven).

41–43]. Such a method cannot accommodate any other explanatory variables, and thus could lead to significantly biased simulation results since the occupant's evacuation sequence is considerably affected by his/her pre-evacuation time, especially in high-deck coaches with dense seat rows as well as a sole and narrow aisle. Furthermore, in high-deck coach evacuations, passengers in each seat row have to first merge into the sole aisle and then move towards the target exit, and the seat location significantly restricts his/her evacuation order, leading to a strong linear relationship between the evacuation time of each passenger and his/her distance to the target exit [1]. These key features of the evacuation process from high-deck coaches are similar to those of high-rise buildings where the effects of different forms of pre-evacuation-time heterogeneity merit further investigation [20]. Though the Cox proportional hazard duration model would be an eligible candidate pre-evacuation time modelling method, it has not been examined by empirical data yet, let alone the quantitative comparison between the two methods. Thus, its efficacy and whether it facilitates higher simulation accuracy remain open problems.

2.3. Overtaking behaviour modelling

Empirical observations suggested that pedestrians with sensitive personality traits prefer overtaking others to following their steps [47], which means that overtaking behaviour is closely related to pedestrian psychology. Accordingly, a body of researchers incorporated psychological characteristics into overtaking behaviour modelling, most of which decomposed the overtaking process into the "lane changing - speed-up - overtaking" action chain, e.g., [24,47,48]. Song, et al. [23] suggested that such an approach fails to reproduce occupants' overtaking behaviour in confined spaces such as aircraft and high-deck coaches. To our best knowledge, the existing passenger evacuation models do not embody overtaking behaviour or their capability has so far remained unproven, except Song et al's work [23], shown in Table 1. In their work, the movement position transition of aircraft passengers in the overtaking process is directly modelled and simulated. And thus it cannot capture the sophisticated manoeuvres (including rotating and lateral movement) performed by passengers while overtaking others in the narrow aisle. Moreover, the movement states of passengers are not updated at each time step, which deviates from the real situations and results in potential biases in simulations.

2.4. Summary

To sum up, this review clearly suggests that a high-deck coach evacuation model framework that is capable of capturing passenger strategic, tactical and operational (locomotion movement and overtaking) behaviours is absent in literature yet, and that the efficacy of the Cox proportional hazard duration model in pre-evacuation time modelling from the perspective of system simulation accuracy and the effects of overtaking behaviour on high-deck coach evacuations are still unclear. As the first effort to fill these gaps, this paper proposes such an integrated framework with three intertwined modules where the Cox proportional hazard duration model is introduced to delineate passenger strategic behaviour and elaborate behavioural rules (e.g., overtaking) are developed and coupled with CPT in the tactical and operational behaviour modules, as well as sheds new light on passenger pre-evacuation and overtaking behaviour modelling and simulation.

3. Model framework development

This section detailedly introduces the strategic-level, tactical-level and operational-level behaviour modules that compose the high-deck coach evacuation model framework.

3.1. Overview of the framework

The high-deck coach evacuation model framework is developed by incorporating the environment and passenger behaviour characteristics into the generic CA models in our previous works [8,33] and thus conforms to the following two well-recognised and widely used assumptions. First, passengers are assumed to realise the interior layout of the high-deck coach so as to create the static floor field for decision-making [30]. It is deemed broadly applicable to high-deck coach passengers due to the straightforward layout in full view of passengers, frequent use of exits and relevant empirical evidence [1,7]. Second, the overlap between passengers and/or obstacles is forbidden [33]. Moreover, the framework is dedicated to the normal evacuation situation without pushing and defined in a two-dimensional discrete

space. The scale of each cell is set as R m $\times$ R m (R=0.1) so as to accurately describe the high-deck coach environment characteristics. Because the empirical data involving Chinese passengers are used for validation, each passenger occupies 4 $\times$ 2 cells according to the body size suggested by [49] (i.e., 0.414 $\times$ 0.206 m^2).

As presented in Fig. 1, the framework is comprised of two layers. In the navigation layer, the static floor field and the static navigation field are constructed to provide the navigation information for passengers' strategic, tactical and operational decision-making in the behaviour layer by using the algorithms in [33] whose details are beyond the scope of this paper. At the onset of evacuations, each passenger experiences a time delay before initiating the evacuation movement, which is predicted by the Cox proportional hazard duration model (strategic-level behaviour module). In the tactical-level behaviour module, a passenger makes an exit choice decision before the evacuation movement begins, which can be revisited and updated when the passenger is confronted with the imbalance between the distance and crowdedness of the candidate exits. The tendency of changing or maintaining the original choice is a joint result of the attractive and repulsive forces. Once the target exit is determined, each passenger moves towards it through adjusting the body posture and updating the movement position, which are delineated by a series of elaborate behavioural rules. In the ensuing sections, details related to the three behaviour modules are respectively described.

3.2. Strategic-level behaviour module

The Cox proportional hazard duration model has numerous variants, depending on the used survival time distribution. However, only the exponential, the Weibull and the Gompertz distributions satisfy the assumption of constant hazard ratios over time [50], among which the Weibull distribution is one of the most common distributions used to capture pre-evacuation times [7] and thus selected. Accordingly, the Cox-Weibull hazard duration model (CWM) is used, and its survival time (T) and hazard function ($h(t_{x_{\mathrm{CWM}}}|x_{\mathrm{CWM}})$) are formulated in Eqs. (1) and (2) [50].

$$T = \left(-\frac{\ln u_{\mathrm{CWM}}}{\exp(\beta_{\mathrm{CWM}} \cdot x_{\mathrm{CWM}})} \right)^{1/\alpha_{\mathrm{CWM}}} \cdot \gamma_{\mathrm{CWM}} \tag{1}$$

$$h(t_{x_{\mathrm{CWM}}}|x_{\mathrm{CWM}}) = \left(\frac{1}{\gamma_{\mathrm{CWM}}} \right)^{\alpha_{\mathrm{CWM}}} \cdot \exp(\beta_{\mathrm{CWM}} \cdot x_{\mathrm{CWM}}) \cdot \alpha_{\mathrm{CWM}} \cdot t_{x_{\mathrm{CWM}}}^{\alpha_{\mathrm{CWM}}-1} \tag{2}$$

Where u_{CWM} is a variable following a uniform distribution $\mathrm{U}(0,1)$; β_{CWM} is the vector of estimable coefficients, and x_{CWM} is the vector of covariates; α_{CWM} and γ_{CWM} are respectively the shape and scale parameters of the Weibull distribution; $t_{x_{\mathrm{CWM}}}$ signifies time.

As suggested by Huang, et al. [1], the distance between passengers and exits is chosen as the sole covariate (x_{CWM}) of the CWM, which is represented by the seat row difference between them. β_{CWM}, α_{CWM} and γ_{CWM} are three key parameters to be calibrated by empirical data.

3.3. Tactical-level behaviour module

Before the evacuation movement, passengers make an exit choice decision, during which distance and crowdedness are two well-recognised influential factors. By using CPT, for each passenger, the probability of choosing a specific exit is determined by the prospect values resulting from distance and crowdedness, described as follows.

For pedestrian n, distance $d_{\mathrm{E}}^{n,e,t}$ is calculated by Eq. (3).

$$d_{\mathrm{E}}^{n,e,t} = M_{\mathrm{H}} - D_{\mathrm{H}}^{n,e,t} \tag{3}$$

Where M_{H} is the maximum distance to evacuate from the high-deck coach; $D_{\mathrm{H}}^{n,e,t}$ denotes the distance of pedestrian n to exit e at t. The distance values are determined by using the static floor field algorithm in [33].

Crowdedness $c_{\mathrm{E}}^{n,e,t}$ describes the potential movement resistance to exit e for pedestrian n at t, given by Eq. (4).

$$c_{\mathrm{E}}^{n,e,t} = \max\left(\frac{N_{\mathrm{E}}^{n,e,t}}{N_{\max}}, \rho_{\mathrm{E}}^{e,t} \right) \cdot \frac{m_{\mathrm{W}}}{w_{\mathrm{E}}^{e}} \tag{4}$$

Where $N_{\mathrm{E}}^{n,e,t}$ is the number of passengers who target at exit e and are closer to it than passenger n at t; $N_{\max}$ is the total number of passengers; $\rho_{\mathrm{E}}^{e,t}$ is the weighted sum of the space and path densities at t (for more details on the calculation method, the reader is referred to [8]); m_{W} is the minimum width of all available exits; w_{E}^{e} is the width of exit e.

Since passengers make decisions according to perception-based uncertain information rather than measurement-based accurate information, the calculated distance and crowdedness values are transformed to the corresponding subjective evacuation outcomes and occurrence probabilities by normalisation, fuzzification and mapping procedures [8]. Then, the cumulative prospect values resulting from distance and crowdedness are determined by the weighting and value functions of CPT [8], which are synthesised by Eq. (5) to generate the overall prospect of exit e. The matter of the prospect value calculation is outside the scope of this paper.

$$P_{\mathrm{E}}^{n,e,t} = r_{c_{\mathrm{E}}}^{n} \cdot P_{c_{\mathrm{E}}}^{n,e,t} + \left(1 - r_{c_{\mathrm{E}}}^{n}\right) \cdot P_{d_{\mathrm{E}}}^{n,e,t} \tag{5}$$

Where $P_{c_{\mathrm{E}}}^{n,e,t}$ and $P_{d_{\mathrm{E}}}^{n,e,t}$ respectively represent the cumulative prospect value induced by distance $d_{\mathrm{E}}^{n,e,t}$ and crowdedness $c_{\mathrm{E}}^{n,e,t}$; $r_{c_{\mathrm{E}}}^{n}$ is the weighting coefficient, set as 0.32 [8].

For passenger n, the probability of choosing exit e is determined by Eq. (6).

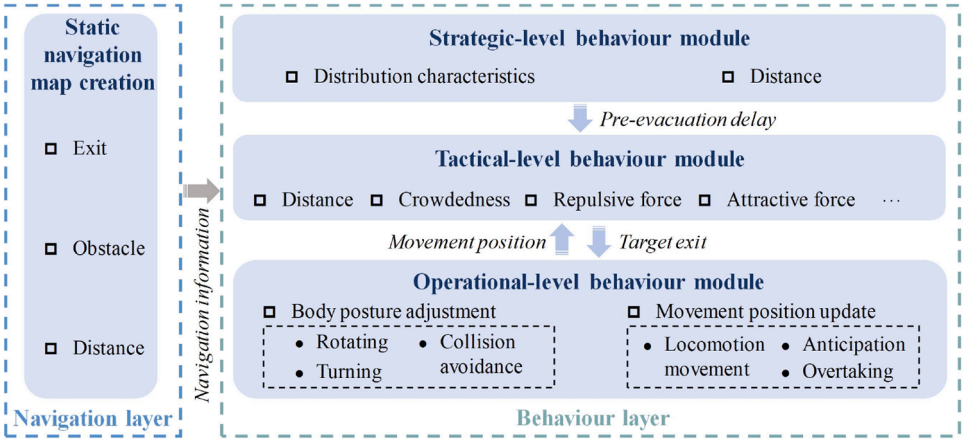

Fig. 1. Overview of the proposed high-deck coach evacuation model framework.

$$P_{\mathrm{E}}^{n,e,t} = \frac{\exp\left(P_{\mathrm{E}}^{n,e,t}\right)}{\sum_j \exp\left(P_{\mathrm{E}}^{n,j,t}\right)} \tag{6}$$

Where $P_{\mathrm{E}}^{n,j,t}$ is the synthetic prospect value of exit j for passenger n at t.

Once the exit choice is determined, passengers initiate the evacuation movement towards the target exit. In this process, they will be given the chance to adjust the exit choice if congestion occurs. The tendency of passengers to revisit the exit choice decision is modelled by the attractive and repulsive forces, given by Eqs. (7) and (8).

$$A^{n,e,t} = C_{\mathrm{A}} \cdot \left(\left(1 - \frac{D_{\mathrm{H}}^{n,e,t}}{M^e}\right) \Big/ 2 + \left(1 - \frac{N^{n,e,t}}{N^{n,e,0}}\right) \Big/ 2 \right)^3 \tag{7}$$

$$R^{n,e,t} = (C_{\mathrm{R}})^{\left(1+N_{\mathrm{EC}}^{n,t}\right)^2} \cdot \left(1 - \exp\left(- \left(\frac{N_{\mathrm{EV}}^{n,t}}{N_{\max}}\right) \cdot \left(\frac{c_{\mathrm{E}}^{n,e,t} - \min\left(c_{\mathrm{E}}^{n,e,t}\right)}{c_{\mathrm{E}}^{n,e,t}}\right)\right)\right) \tag{8}$$

Where C_{A} and C_{R} are the coefficients, set as 0.2 and 0.4 respectively [8]; M^e is the maximum distance to target exit e; $N_{\mathrm{EC}}^{n,t}$ represents the number of changing the exit choice for passenger n at t; $N_{\mathrm{EV}}^{n,t}$ denotes the number of evacuated passengers at t.

3.4. Operational-level behaviour module

When the pre-evacuation delay has passed and the target exit is determined, each passenger can move to the unoccupied neighbouring cells along one of the four candidate directions or stay still at each time step. The position of passengers is updated in parallel, by the use of the Neumann neighbourhood [30].

3.4.1. Overview of the module

Except for the movement position update, high-deck coach passengers also frequently adjust their body postures to manoeuvre through confined spaces in evacuations [1]. Thus, three behaviours concerning body posture adjustment (i.e., rotating, turning and collision avoidance) and three behaviours related to movement position update (i.e., locomotion movement, anticipation and overtaking) are introduced to comprehensively embody the operational behavioural characteristics of high-deck coach passengers.

Fig. 2 presents an overview of the implementation procedures, which will be repeated until all passengers have evacuated. According to whether passengers face the aisle straightforwardly or sideways, two types of body postures (vertical or horizontal) are identified (visualised in Fig. 3), which result in a series of different manoeuvres. Thus, shown in the left grey block of Fig. 2, at the beginning of each time step, the body posture of each passenger is first checked to determine whether he/she is eligible to rotate the body. Then, for those passengers who potentially collide with others or prepare to enter the stairways, the collision avoidance or turning behaviour is conducted.

As shown in the right blue block of Fig. 2, after the manoeuvres related to body posture adjustment, the possibility of updating the position will be checked for each passenger. To delineate passengers' overtaking behaviour, two sorts of personalities, radical and non-radical, are introduced [47]. When confronted with congestion, non-radical passengers are patient and follow the steps of the persons in front, whereas radical passengers are impatient and always seek for the opportunity to overtake others. It should be noted that passengers who have performed the overtaking behaviour will not be given the opportunity to make a locomotion movement decision, as this behaviour essentially involves both body posture and movement position changes. After determining the intended movement direction, each passenger performs the anticipation behaviour to avoid potential gridlock, and finally only the eligible passengers are allowed to implement the movement.

3.4.2. Body posture adjustment

Before updating the movement position, each passenger will first adjust his/her body posture according to the surrounding situations, which only occurs when the required cells for repositioning are empty. Note that pedestrians will not move forwards regarding physical position thereof.

(1) Rotating behaviour

Generally, passengers face towards the desired direction when moving to the aimed exit [28]. Thus, the rotating behaviour would occur when passenger n's orientation deviates from his/her desired direction, which is determined by the rotating probability P_{R}^n in Eq. (9).

$$P_{\mathrm{R}}^n = \frac{\omega^n \cdot R}{v_{\max} \cdot \theta_{\mathrm{R}}^n} \tag{9}$$

Where ω^n is the angular speed of passenger n, set as 2 π/s [8]; R represents the length scale of discrete space, the value of which is 0.1 m; $v_{\max}$ denotes the maximum desired velocity of the system of passengers, set as 2 m/s [8]; $\theta_{\mathrm{R}}^n = \frac{\pi}{2}$ is the rotating angle.

As illustrated in Fig. 3, the rotating direction can be anti-clockwise or clockwise, depending on passenger n's desired direction ($\overrightarrow{D}_{\mathrm{P}}^n$) and the

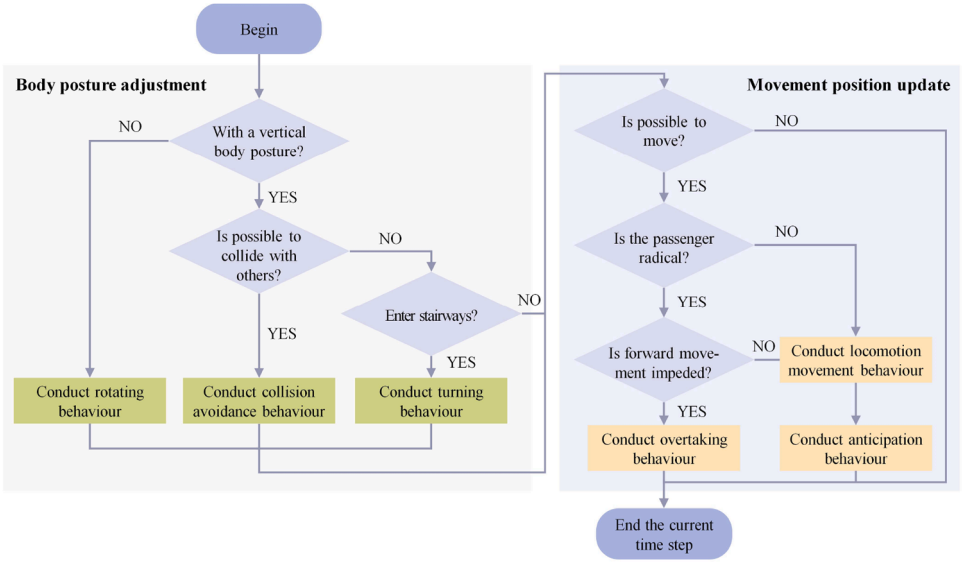

Fig. 2. Flow chart of the operational-level behaviour module.

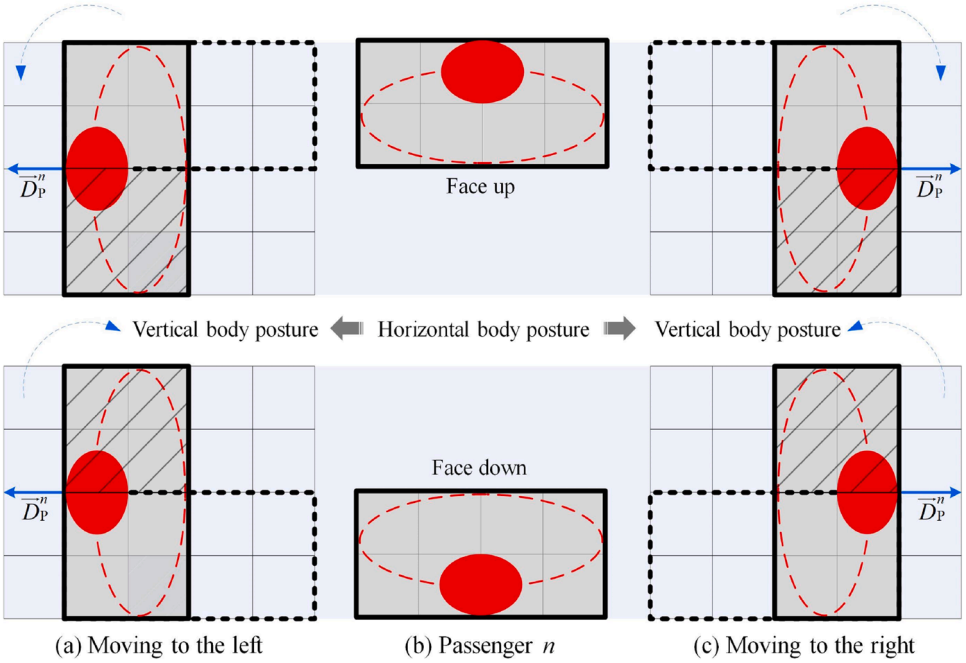

Fig. 3. Rotating behaviour of passengers. The aisle area is marked in light blue. The black dotted frame in (a) and (c) represents the position of passenger n before rotating his/her body. The hatched lines are superposed onto the cells necessary for this behaviour.

face position. Four empty cells are required for performing this manoeuvre.

(2) Turning behaviour

Before entering the stairways from the aisle, each passenger will first turn the body to adjust the orientation to face the exit [1,51]. Thus, the trigger condition of the turning behaviour is whether the passenger prepares to enter the stairways. An example of the turning behaviour is used to illustrate the related rules, as shown in Fig. 4. If one or more required cells (eight in total) are occupied by any other passengers or obstacles, passenger n will stay still until all these cells are available.

(3) Collision avoidance behaviour

Within the narrow aisle in high-deck coaches, if there is a passenger with an opposite moving direction on passenger n's path to the aimed exit, a collision between them will potentially occur. In this case, passengers with the vertical body posture will rotate their bodies according to the inverse process in Fig. 3 to clear space for their movement in order to avoid the oncoming collision [1,51]. For each desired direction $\overrightarrow{D}_{\mathrm{P}}^{n}$ (moving to the lelft or right), one of the two inverse rotating processes in Fig. 3 is randomly conducted. It is logically understandable that the shorter the distance between two passengers with opposite moving directions is, the stronger the tendency of this behaviour is, given by Eq. (10).

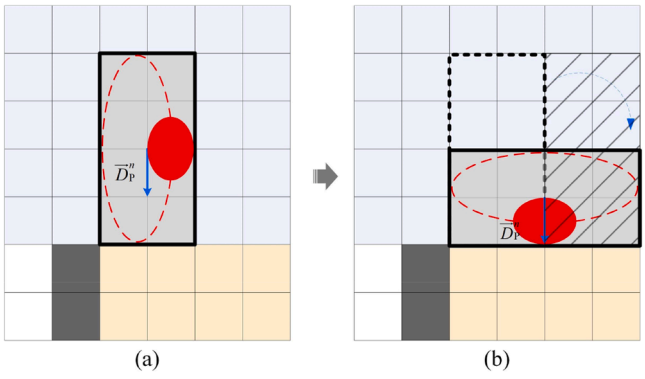

Fig. 4. Turning behaviour of passenger n. The aisle area and the stairway area are respectively marked in light blue and orange. The black cells represent obstacles. The hatched lines are superposed onto the cells required for this behaviour.

$$P_{\mathrm{C}}^{n}=\left(1-2\cdot d_{\mathrm{O}}^{n,j}\right)\cdot\exp\left(d_{\mathrm{O}}^{n,j}\right) \tag{10}$$

Where $d_{\mathrm{O}}^{n,j}$ is the distance between passengers n and j who move oppositely.

It should be noted that the collision avoidance behaviour will be triggered only when passenger j enters into passenger n's intimate space, i.e., $d_{\mathrm{O}}^{n,j}\leq 0.5$ m, which is consistent with the findings from [52].

3.4.3. Movement position update

After adjusting the body posture, with velocity $v^{n,t}$, passenger n has a probability of $v^{n,t}/v_{\max}$ to update the movement position at each time step.

(1) Locomotion movement behaviour

At time step t, to adapt to the changing environment, the passengers moving on the flat floor adjust his/her movement velocity according to Eq. (11) [53].

$$v^{n,t}=v_{\mathrm{F}}^{n}\cdot\left(1-\exp\left(-\varkappa\cdot\left(\frac{1}{\rho^{n,t}}-\frac{1}{\rho_{\max}}\right)\right)\right)\cdot\eta^{n,t}\cdot\eta_{\mathrm{LC}}^{n} \tag{11}$$

With

$$v_{\mathrm{F}}^{n}=\begin{cases}-0.001\cdot A^{n}+0.879\cdot H^{n}-0.003\cdot W^{n}\ \textit{for females}\\ -0.001\cdot A^{n}+0.486\cdot H^{n}-0.001\cdot W^{n}\ \textit{for males}\end{cases} \tag{12}$$

Where v_{F}^{n} represents the free velocity of passenger n, which is correlated with his/her age (A^n), height (H^n) and weight (W^n) [54]; $\varkappa$=1.913 is a factor; $\rho^{n,t}$ is the density within passenger n's visual range (set as 2 m [8]) at time step t, and $\rho_{\max}$ is the maximum density; $\eta^{n,t}$ and η_{LC}^{n} are respectively the velocity reduction factor related to the seat cushion area and the lighting condition ($\eta^{n,t}=0.5$, if passenger n occupies at least one seat cushion cell; 1, otherwise. For the normal and dim lighting conditions, η_{LC}^{n} is set as 1 and 0.88 respectively [1]).

The locomotion movement behaviour essentially concerns the choice of the movement direction, which is also delineated by CPT according to the distance and crowdedness information perceived by passengers. For

pedestrian n, the distance of each candidate movement direction ($\overrightarrow{D}^{k}$) to exit e is calculated by Eq. (13).

$$d_{\mathrm{M}}^{n,k}=\frac{1}{N\left(\Omega_{\mathrm{VZ}}^{n,k}\right)}\sum_{\left(x_{\mathrm{VZ}}^{n,k},y_{\mathrm{VZ}}^{n,k}\right)\in\Omega_{\mathrm{VZ}}^{n,k}}F_{\mathrm{H}}^{e,\left(x_{\mathrm{VZ}}^{n,k},y_{\mathrm{VZ}}^{n,k}\right)} \tag{13}$$

Where $\Omega_{\mathrm{VZ}}^{n,k}$ denotes a set that contains cells $(x_{\mathrm{VZ}}^{n,k},y_{\mathrm{VZ}}^{n,k})$ within a visual zone bisected by $\overrightarrow{D}^{k}$, which is modelled as a cone, with an angle of $\pi/2$ and a length of 2 m [8]; $F_{\mathrm{H}}^{e,\left(x_{\mathrm{VZ}}^{n,k},y_{\mathrm{VZ}}^{n,k}\right)}$ represents the static floor field value of cell $(x_{\mathrm{VZ}}^{n,k},y_{\mathrm{VZ}}^{n,k})$ to exit e.

Crowdedness $c_{\mathrm{M}}^{n,k}$ depicts the overall movement resistance of passenger n to exit e, calculated by Eq. (14).

$$c_{\mathrm{M}}^{n,k}=\left(c_{\mathrm{MC}}^{n,k,1}+c_{\mathrm{MC}}^{n,k,2}+c_{\mathrm{ML}}^{n,k}\right) \tag{14}$$

Where $c_{\mathrm{MC}}^{n,k,1}$ and $c_{\mathrm{MC}}^{n,k,2}$ are the two cell-level movement resistance elements, and $c_{\mathrm{ML}}^{n,k}$ is the lane-level movement resistance element. For more detailed descriptions of the definitions and calculation methods, the reader is referred to [8].

Then, the same procedures in Section 3.3 are used to obtain the cumulative prospect values induced by distance and crowdedness, based on which the probability of moving towards candidate direction $\overrightarrow{D}^{k}$ is determined, shown in Eq. (15).

$$\begin{cases} w_{\mathrm{M}}^{n,k}\cdot\prime_{\mathrm{M}}^{n,k} & \#moving\ towards\ \overrightarrow{D}^{k} \\ 1-\sum_{k}\prime_{\mathrm{M}}^{n,k} & \#staying\ still \end{cases} \tag{15}$$

With

$$\prime_{\mathrm{M}}^{n,k}=\frac{\exp\left(P_{\mathrm{M}}^{n,k}\cdot\zeta^{n,k}\right)}{\sum_{j}\exp\left(P_{\mathrm{M}}^{n,j}\cdot\zeta^{n,j}\right)} \tag{16}$$

$$P_{\mathrm{M}}^{n,k}=r_{d_{\mathrm{M}}}^{n}\cdot P_{d_{\mathrm{M}}}^{n,k}+\left(1-r_{d_{\mathrm{M}}}^{n}\right)\cdot P_{c_{\mathrm{M}}}^{n,k} \tag{17}$$

Where $w_{\mathrm{M}}^{n,k}=\exp(-0.09|\theta_1|)$ is an inertia effect factor related to the deviation (θ_1) between the desired direction ($\overrightarrow{D}_{\mathrm{p}}^{n}$) and the candidate movement direction ($\overrightarrow{D}^{k}$) [55]; $P_{\mathrm{M}}^{n,k}$ is the prospect values of direction $\overrightarrow{D}^{k}$ in relation to distance ($P_{d_{\mathrm{M}}}^{n,k}$) and crowdedness ($P_{c_{\mathrm{M}}}^{n,k}$), and $r_{d_{\mathrm{M}}}^{n}$ is the weighting coefficient, set as 0.7 [8]; $\zeta^{n,k}$ is a factor that describes passengers' tendency to avoid occupying the seat cushion cells which will slow down the pedestrian movement. $\zeta^{n,k}=0.5$, if at least one of the neighboring cells in direction $\overrightarrow{D}^{k}$ belongs to the seat cushion cells; 1, otherwise.

In case of a conflict where two or more passengers have the same target cell, one of the passengers is randomly selected to implement the movement. Moreover, as observed in our experiments [1,51], passengers usually bend down and lower their heads for reasons of safety and the movement demand when stepping on the stairways. Accordingly, the body size of passengers is extended to 4 × 3 cells in this process, which is further justified by the consistency of the maximum density between simulations and experiments. Also, when exiting through the emergency door, some typical behaviours of passengers such as hesitation and preparation are observed to lead to an average time delay of 1.15 s [1,7], which is introduced in this module to depict such a behavioural characteristic.

(2) Anticipation behaviour

Due to the confined space, gridlock could occur when passengers from different directions merge (e.g., entering the aisle). In real life, passengers usually judge the prospective movement of others and yield to those in a favourable position so as to avoid potential gridlock in advance [1,51], which is referred to as anticipation behaviour. To illustrate the related rules, the merging process from the seat area into the aisle is used as an example, presented in Fig. 5. Passengers n and j compete for space to enter the aisle so as to move to the target exit in front, and gridlock is potentially formed (see Fig. 5 (c)) if their positions are updated according to their intended locomotion movement decisions (see Fig. 5 (b)), which can be anticipated via communication or body actions. To avoid it, only the passenger with the largest body area that has entered into the target space (herein the aisle) at the current time step is allowed to implement the movement (see Fig. 5 (d)).

(3) Overtaking behaviour

As aforementioned, when the forward movement of radical passengers is impeded by others in front, they will invariably conduct the overtaking behaviour rather than wait in the queue as long as the overtaking condition is satisfied. To overtake others in the narrow aisle of high-deck coaches, sophisticated manoeuvres, including rotating and lateral movement, are essential. Thus, elaborate behavioural rules are designed to comprehensively capture passengers' overtaking behaviour.

As illustrated in Fig. 6, when the forward movement of radical passenger j is blocked by passenger n, passenger j will perform the overtaking behaviour. Four types of overtaking situations are identified according to the relative position relations between passengers j and n. Generally, overtaking behaviour is accompanied by the acceleration action [48], and thus passengers move forwards two cells in the overtaking process. This means that the movement velocity of passengers while conducting overtaking behaviour is twice as fast as that of other passengers, which is consistent with the existing studies [23,24]. After the manoeuvres in Fig. 6, passenger j is possible to overtake passenger n in the next time steps. The proportion of radical passengers in simulations is denoted as P_{N}^{r}.

4. Simulation setups

The three parameters of the CWM in the strategic behaviour module will be calibrated by using the maximum likelihood method (for more details, see Supplementary material A). As for the tactical and operational behaviour modules, the decision-making parameter values in [8] are used, and the simulation results evidence the applicability of these values. Thus, the key parameter values of the framework are all determined.

Thereafter, three parts of simulation analyses are conducted. First, 13 typical high-deck coach evacuation scenarios are simulated by the integrated framework, the results of which are compared to the empirical data and those from the widely used passenger evacuation simulation software, i.e., Pathfinder (as indicated in Section 2). Second, comparisons between the simulation outcomes of the frameworks using the CWM and the Weibull probabilistic distribution (WD, the stochastic approach based on the probabilistic distribution) are conducted to evaluate the efficacy of the two approaches from the perspective of the prediction accuracy of the entire framework. Third, systematic simulation analyses are performed to reveal the effects of overtaking behaviour on high-deck coach evacuations. 30 runs are repeated for each simulation according to the quantitative analyses by using the convergence measures in [56].

4.1. Validation of the proposed framework

The proposed framework is validated by using an empirical data-set in [7], which is collected from 29 full-scale controlled experiments, involving two widely used high-deck coaches and 13 typical evacuation scenarios with different available exits, age groups and lighting conditions, shown in Table 2.

To make a credible comparison between simulation and experiment, the geometry of high-deck coaches A and B in simulations is constructed by using a fine spatial discretisation (0.1 m × 0.1 m) according to their geometrical structures, shown in Fig. 7. The seat arrangement of

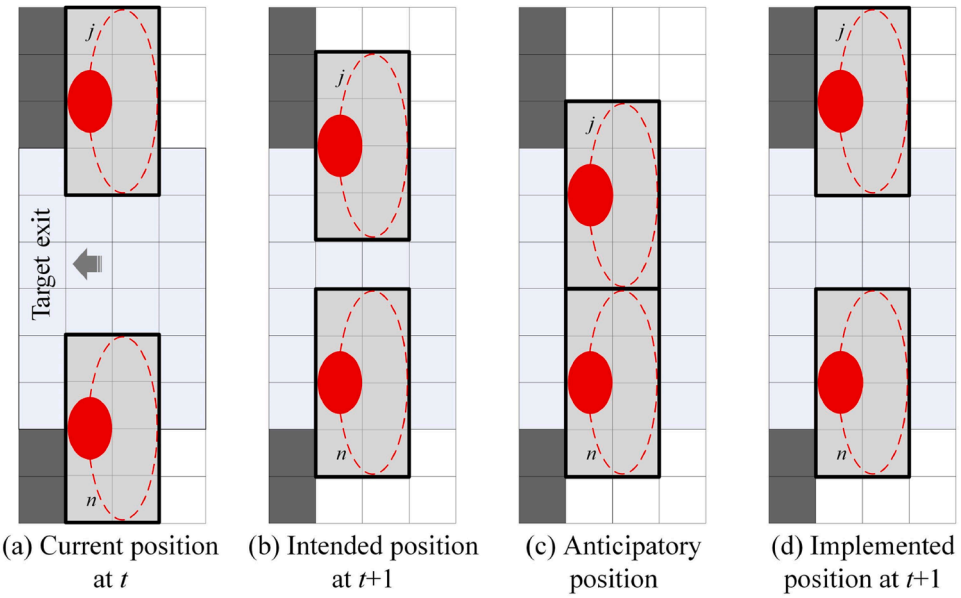

Fig. 5. Anticipation behaviour of passengers *n* and *j*. The aisle area is marked in light blue, and the black cells represent the seat backs, which are impassable.

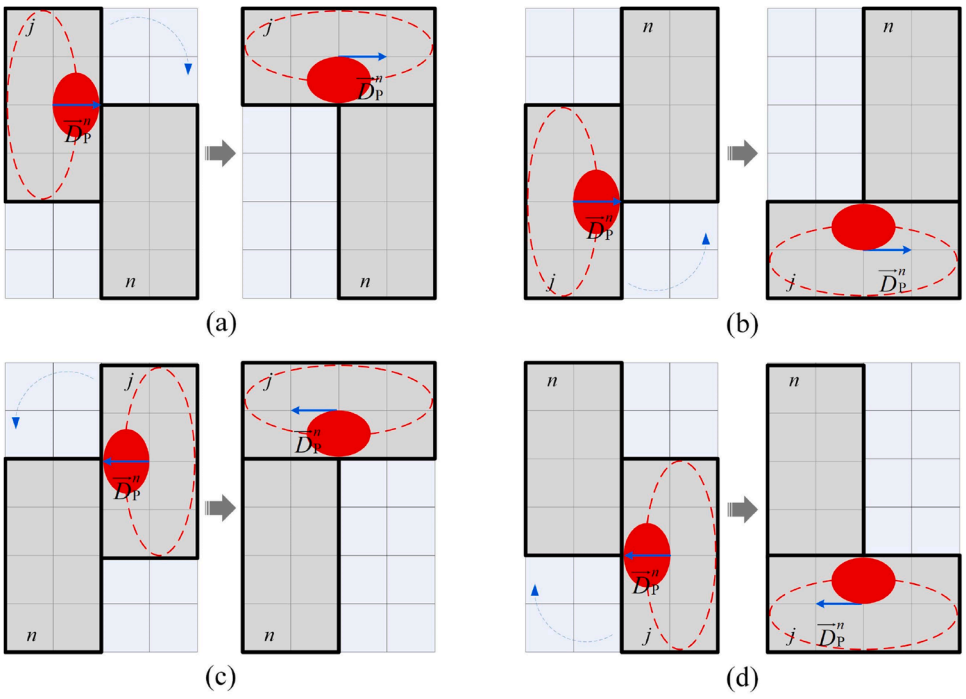

Fig. 6. Overtaking behaviour of passengers.

passengers in simulations exactly corresponds to that of experiments. Moreover, based on the physical attributes of different geometry components, three kinds of areas are identified, i.e., the normally passable area, the movement slowdown area, and the impassable area (see Fig. 7). Based on the rigorous frame-by-frame video observations, the proportion of radical passengers in simulations (P_N^r) is set as 0 to accord with the ordered evacuation phenomenon observed in experiments [1,7] (also demonstrated by Fig. 12). To ensure a fair comparison, the same geometric structure and simulation parameters are used in the Pathfinder model. The related details are described in Supplementary material B.

Thereafter, simulations are conducted by using the proposed framework and the Pathfinder model under the same evacuation conditions as that of experiments. To systematically validate the proposed framework, four commonly used indicators of evacuation behaviour, i.e., evacuation time, alighting time gap, flow rate and exit choice, are collected and compared with those from experiments and the Pathfinder model.

Evacuation time. The cumulative evacuation time curves (macroscopic) and the spatial distribution of passenger evacuation times (mesoscopic) are derived for the 13 scenarios. Four metrics related to the evacuation time curve in [57], i.e., the Euclidean Relative Difference (ERD), the Euclidean Projection Coefficient (EPC), the Secant Cosine (SC) and the difference of the total evacuation time (DTET), are used to quantitatively evaluate the model performance. Specifically, ERD measures the average distance between simulated and observed data. EPC is

Table 2
Evacuation scenarios used for validation.

Scenario number	High-deck coaches	Available exits	Age Groups	Lighting conditions
1	A	FR	MG	N
2		F	MG	N
3		R	MG	N
4	B	FRE	ST	D
5		FR	ST	D
6		F	ST	D
7		R	ST	D
8		E	ST	D
9		FR	MA	D
10		F	MA	D
11		E	MA	D
12		FR	MA	N
13		FR	ST	N

The acronyms identify the available exits (FRE = front-rear-and-emergency door, FR = front-and-rear door, F = front door, R = rear door, and E = emergency door), age groups (MG = mixed age group, MA = middle-aged people, and ST = young students), and lighting conditions (N = normal lighting condition, and D = dim lighting condition).

an indicator of the best possible coincidence degree between the simulated and observed curves. SC provides a measure of how well the shape of the simulated curve matches that of the observed curve. For a more detailed description of the calculation methods, the reader is referred to [57]. The perfect match between the experimental and simulated evacuation time curves leads to the optimal value of these four metrics, i.e., $ERD = 0$, $EPC = 1$, $SC = 1$, and $DTET = 0$. According to the suggestion in [57], the acceptance criterion of these four metric values for the model validation is: $ERD \leq 0.25$, $0.8 \leq EPC \leq 1.2$, $SC \geq 0.8$, and $DTET \leq 0.15$.

Alighting time gap. A total of 11 alighting time gap samples are collected from 13 evacuation scenarios by using the method in [7], and statistical comparisons between the distribution characteristics (mesoscopic) of the samples from experiments, our framework and the Pathfinder model are conducted.

Flow rate. Similarly, a total of 17 instantaneous flow rate samples are obtained. Then, the distribution characteristics (mesoscopic) of each sample from our framework are statistically compared to those from experiments and the Pathfinder model.

Exit choice. The exit shares (macroscopic) and the spatial distribution of passenger exit choices (mesoscopic) from experiments, our framework and the Pathfinder model in multi-exit evacuation scenarios are measured and compared.

In light of the following three reasons, microscopic metrics, e.g., trajectories, are not involved in the validation [33]. First, evacuation simulation models are prevailingly deployed to estimate the macroscopic and mesoscopic properties of the facility. Second, validating using microscopic metrics does not necessarily lead to a macroscopically and mesoscopically valid model. Third, for high-deck coach evacuation scenarios, the microscopic empirical data such as trajectories are currently unavailable in literature [7].

4.2. Performance comparisons of two pre-evacuation time modelling approaches

Simulations of the 13 evacuation scenarios are also performed by using the framework with the WD, and the evacuation time, alighting time gap, flow rate and exit choice are measured to comprehensively and quantitatively compare the prediction performance of the frameworks using the CWM and the WD. According to the parameter estimation using the empirical pre-evacuation time data in [1], the shape and scale parameter values of the used WD are respectively 14.61 and 2.26.

4.3. Effects of overtaking behaviour

To explore the effects of overtaking behaviour on evacuation efficiency and crowdedness, one of the risky scenarios with only one door available [1], B_R_ST_D, is taken as an illustrative example to perform simulation analyses. As indicated in Section 3.4, the number of overtaking behaviour is dependent on the proportion of radical passengers (P_N^r). Accordingly, the value of P_N^r is changed by a small time step (i.e., 25 %) to continuously adjust the number of overtaking behaviour (see Fig. C.1 in Supplementary material C) while keeping the values of other parameters constant. In this process, the passenger evacuation time, the

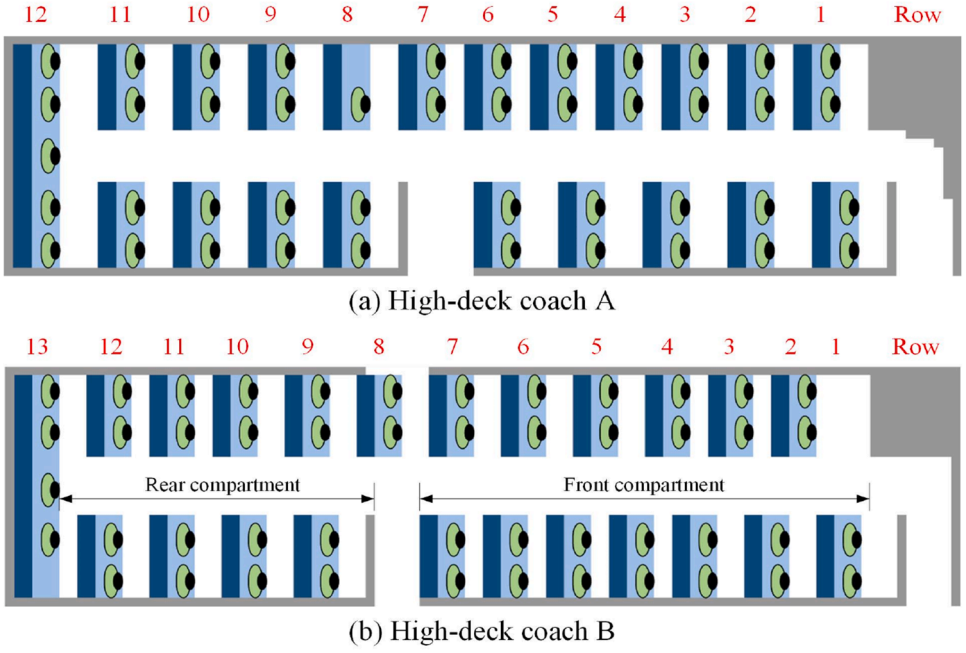

Fig. 7. Layout of high-deck coaches A and B. The white colour denotes the normally passable area, and the light blue colour represents the seat cushion area where the passenger movement is slowed down. The impassable area is coloured in grey and deep blue, consisting of coach body panels, seat backs, and so on.

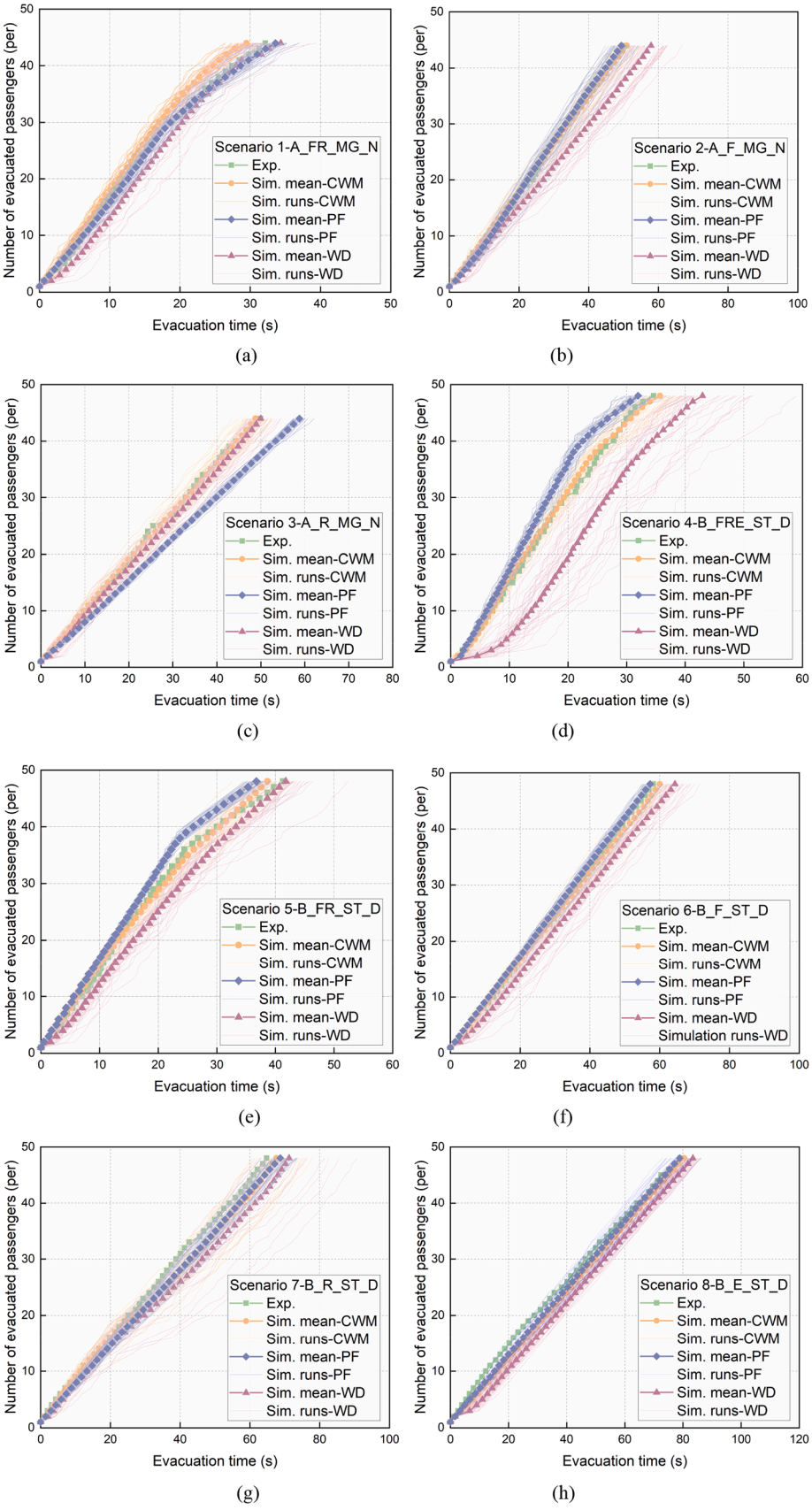

Fig. 8. Comparison of the experimental and simulated evacuation time curves. The experimental result is shown by using the thick green line with squares. The thick orange line with circles, the thick brown line with triangles and the thick purple line with diamonds respectively represent the simulated result averaged over 30 runs by using the framework with the CWM, the Pathfinder model (PF), and the framework with the WD.

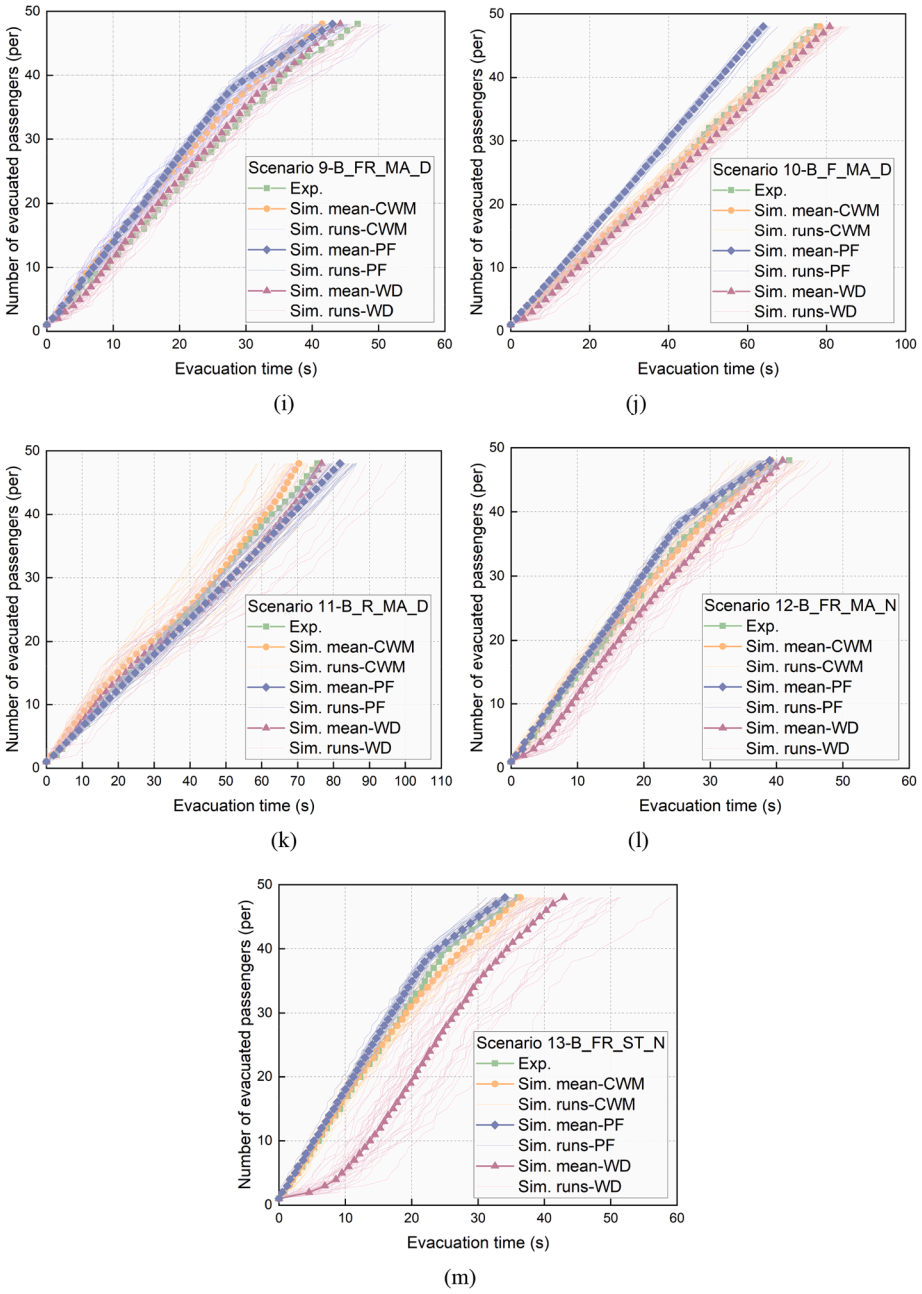

Fig. 8. (*continued*).

average maximum linear density (AMLD) and the cumulative linear density (CLD) within the aisle, as well as the density distribution (DD) are measured. Thus, the cumulative evacuation time curves (macroscopic) and the spatial distribution of passenger evacuation times (mesoscopic) are obtained. To compute the other two macroscopic metrics (the AMLD and CLD) and one mesoscopic metric (the DD), the high-deck coach carriage is divided into the front and rear compartments (see Fig. 7 (b)).

Average maximum linear density (AMLD). it is defined as the mean of the instantaneous linear density values in the stable phase [1], which is the period when the linear density of the aisle fluctuates around the maximum value.

Cumulative linear density (CLD). it is the integral value of the instantaneous linear density and time [1].

Density distribution (DD). the density of each cell is defined as the time (in percentage) it is occupied during evacuations [33].

5. Results

This section presents the results of the conducted simulation analyses to show that the proposed framework is capable of reproducing high-deck coach passenger evacuation behavioural characteristics in various scenarios and exhibits significant advantages over the Pathfinder model, and to demonstrate that the CWM facilitates a substantial improvement in the prediction accuracy of the entire framework when compared with the WD, as well as to elucidate the effect of passenger overtaking behaviour on high-deck coach evacuations.

5.1. Validation of the proposed framework

To facilitate the performance comparison, some results from the frameworks using the CWM and the WD, and the Pathfinder model are visualised together, whereas analyses related to the comparison between

the CWM and the WD will be provided in the next section.

5.1.1. Evacuation time

Fig. 8 presents the observed and simulated evacuation time curves for the 13 scenarios. It can be clearly seen that in all the 13 scenarios, the evacuation time curves from our framework (using the CWM) are close to those from experiments, and the degree of match of our results is significantly higher than that of the Pathfinder model (PF) when compared with the observed one. To quantify the coincidence degree between the simulated and observed evacuation time curves, four metrics (SC, ERD, EPC and DTET) are calculated and shown in Table 3. It can be found that the metric values of our framework (using the CWM) are close to the optimal values and satisfy the validation criteria for all the 13 scenarios, whereas those of the Pathfinder model do not meet the acceptance criteria in two scenarios. The prediction errors related to the four metrics are provided in Table 4. It shows that the errors of our framework (using the CWM) are all smaller than that of the Pathfinder model except the four cases (denoted by the sign (*)), with an average of 11.90 % improvement in the prediction performance.

Regarding the spatial distribution of passenger evacuation times, as presented in Fig. 9, compared with the Pathfinder model, the results from our framework (using the CWM) are generally closer to those from experiments. For quantitative comparisons, Table 5 shows the descriptive statistics of the related simulation errors, which are assessed by the absolute difference between the simulated and observed values. It can be clearly seen that the errors of our framework (using the CWM) are all smaller than that of the Pathfinder model except the few cases (denoted by the sign (*)), with an average of 14.50 % reduction. The paired-samples t-tests between the simulated and observed average evacuation times of each seat row are conducted, and the results are listed in Table 6. It shows that regardless of the significance level (5 % or 1 %), there is no statistically significant difference between the results from our framework (using the CWM) and experiments, whereas a statistically distinct discrepancy is respectively observed in four scenarios and one scenario at the significance level of 5 % and 1 % for the Pathfinder model.

These results demonstrate that the proposed framework is capable of reproducing the macroscopic and mesoscopic characteristics of passenger evacuation times in various high-deck coach evacuation scenarios and is superior to the Pathfinder model, with the prediction errors reduced by an average of 13.20 %.

5.1.2. Alighting time gap

The descriptive statistics of the 11 alighting time gap samples from experiments and simulations are shown in Table C.1 (see Supplementary material C). To statistically examine the coincidence degree between the observed and simulated samples, the non-parametric hypothesis tests between the paired samples are conducted by using the Mann-Whitney-Wilcoxon (MWW) test, the Two-sample Kolmogorov-Smirnov (K-S) test and the Welch's t-test (Welch) [1], shown in Table 7. It shows that at the significance level of 5 %, all alighting time gap samples of our framework (using the CWM) show no statistically significant difference from those of experiments, with the null hypothesis accepted in at least one test, whereas only 7 alighting time gap samples of the Pathfinder model match with the empirical data. Also, for the proposed framework, the total number of acceptances of the null hypothesis is much more than that of the Pathfinder model (25 vs. 14). These results demonstrate that the proposed framework is capable of reproducing the alighting time gap distribution characteristics of high-deck coach passengers in various scenarios and is superior over the Pathfinder model, with the prediction errors reduced by 34.85 % on average.

Table 4
Performance comparison results of the framework using the CWM and the Pathfinder model based on the prediction error from the four metrics related to the evacuation time curve.

Scenario	CWM	PF	Ratio=(CWM-PF)/PF
A_FR_MG_N	0.338	0.145	**1.331***
A_F_MG_N	0.101	0.095	**0.064***
A_R_MG_N	0.131	0.622	**-0.789**
B_FRE_ST_D	0.226	0.521	**-0.566**
B_FR_ST_D	0.186	0.422	**-0.559**
B_F_ST_D	0.109	0.092	**0.185***
B_R_ST_D	0.217	0.234	**-0.073**
B_E_ST_D	0.178	0.103	**0.728***
B_FR_MA_D	0.438	0.487	**-0.101**
B_F_MA_D	0.065	0.409	**-0.841**
B_R_MA_D	0.211	0.251	**-0.159**
B_FR_MA_N	0.201	0.318	**-0.368**
B_FR_ST_N	0.147	0.242	**-0.393**
	Avg.		**-0.119**

For each scenario, the error value in Table 4 is defined as the sum of the prediction error (|simulated value − optimal value|) of each metric.

5.1.3. Flow rate

The descriptive statistics of the 17 instantaneous flow rate samples from experiments and simulations are shown in Table C.2 (see Supplementary material C). Similarly, three non-parametric hypothesis tests are used to statistically measure the degree of match between the simulated and observed samples, as presented in Table 8. The null hypothesis is that there is no significant difference between the paired samples. It can be found that at the significance level of 5 %, 14 flow samples of our framework (using the CWM) and 13 flow samples of the Pathfinder model show no statistically significant difference from those of experiments, with the acceptance of the null hypothesis in at least one test, which results in a total of 33 and 27 acceptance results for the null

Table 3
Validation metric values related to the evacuation time curve, where the symbol indicates whether the validation criteria are satisfied ($\surd$ = satisfied, and × = not satisfied).

Scenario	SC		ERD		EPC		DTET		Satisfaction	
	CWM	PF	CWM	PF	CWM	PF	CWM	PF	CWM	PF
A_FR_MG_N	0.950	0.960	0.098	0.035	1.106	0.975	0.084	0.045	$\surd$	$\surd$
A_F_MG_N	0.958	0.950	0.029	0.027	0.990	1.013	0.020	0.018	$\surd$	$\surd$
A_R_MG_N	0.927	0.940	0.031	0.211	0.989	0.827	0.016	0.178	$\surd$	×
B_FRE_ST_D	0.854	0.860	0.038	0.144	1.010	1.156	0.032	0.076	$\surd$	$\surd$
B_FR_ST_D	0.935	0.933	0.046	0.115	1.010	1.130	0.065	0.110	$\surd$	$\surd$
B_F_ST_D	0.979	0.981	0.031	0.031	0.974	1.026	0.031	0.016	$\surd$	$\surd$
B_R_ST_D	0.966	0.967	0.075	0.075	0.935	0.934	0.043	0.060	$\surd$	$\surd$
B_E_ST_D	0.972	0.978	0.076	0.048	0.944	0.969	0.018	0.002	$\surd$	$\surd$
B_FR_MA_D	0.922	0.896	0.118	0.144	1.128	1.158	0.114	0.081	$\surd$	$\surd$
B_F_MA_D	0.973	0.975	0.018	0.176	0.990	1.213	0.010	0.175	$\surd$	×
B_R_MA_D	0.965	0.981	0.061	0.077	1.047	0.929	0.068	0.084	$\surd$	$\surd$
B_FR_MA_N	0.899	0.896	0.034	0.072	1.001	1.072	0.065	0.070	$\surd$	$\surd$
B_FR_ST_N	0.952	0.964	0.051	0.075	0.963	1.077	0.011	0.054	$\surd$	$\surd$

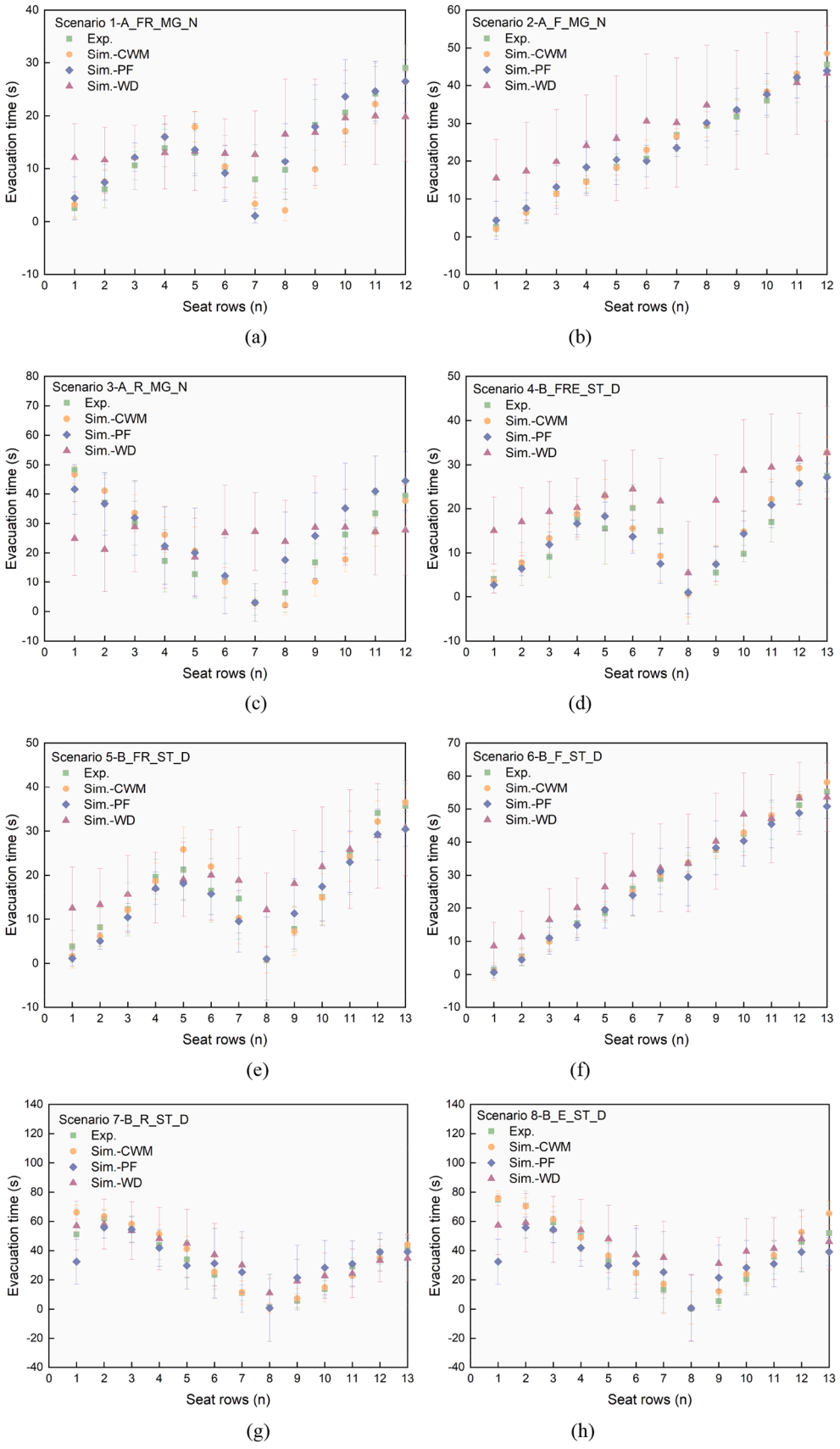

Fig. 9. Spatial distribution of passenger evacuation times against the seat row number from simulations and experiments.

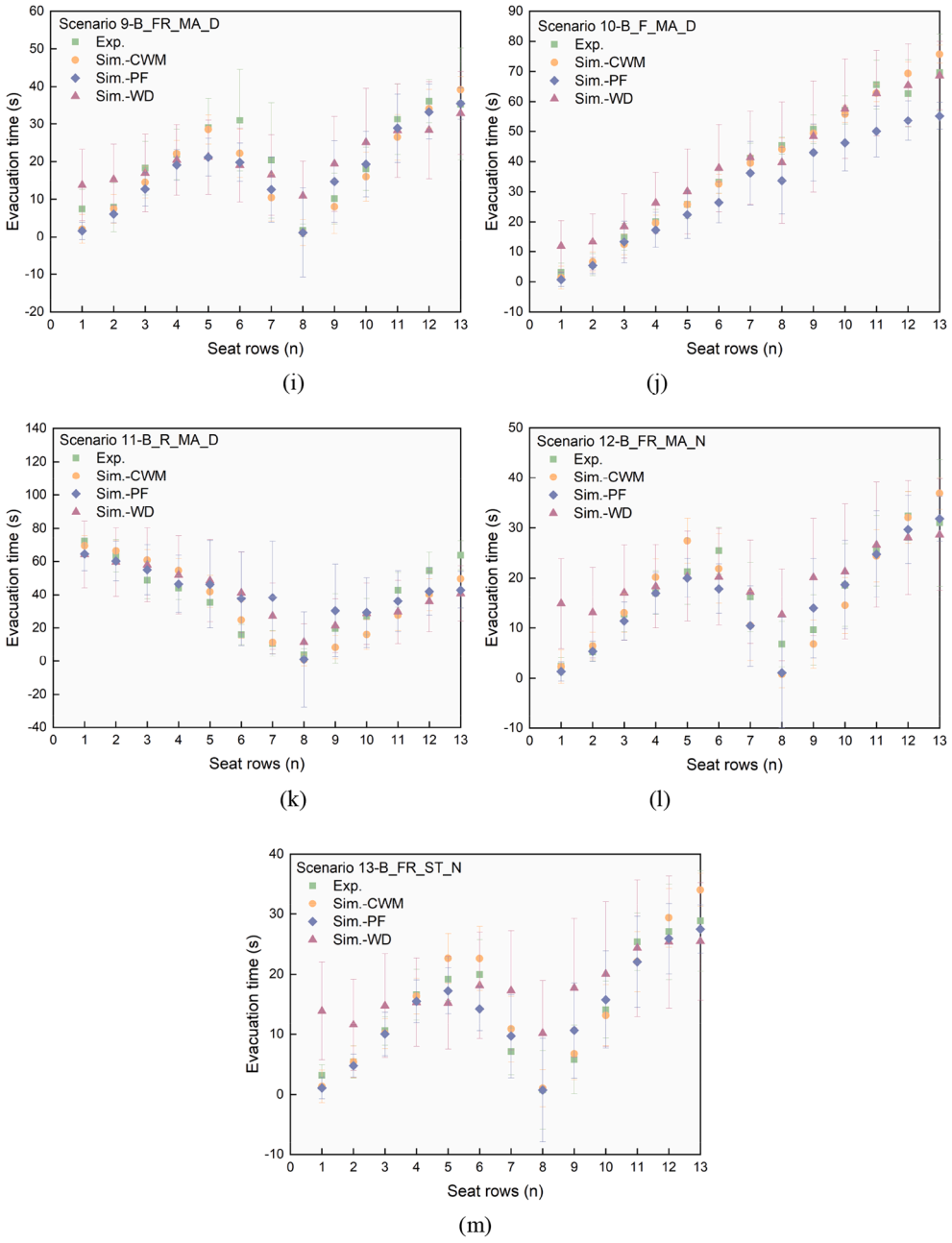

Fig. 9. (*continued*).

hypothesis respectively. The remaining discrepancies between the simulated and experimental results should be attributed to the other factors that are not considered in the proposed framework, e.g., the group behaviour. These results suggest that the proposed framework is able to accurately predict the instantaneous flow rate distribution characteristics of high-deck coach passengers in manifold scenarios and outperforms the Pathfinder model, with an 8.82 % improvement in the prediction performance on average.

5.1.4. Exit choice

As illustrated in Fig. 10, the exit shares from our framework (using the CWM) and the Pathfinder model well coincide with those observed in experiments, with the average of the absolute difference less than 5 %. At the mesoscopic level, the spatial distribution of passenger exit choices from simulations is consistent with those from experiments, shown in Fig. 11. Also, it can be found that the results from these two models are close, which could be because the rather confined high-deck coach carriage restricts passengers' exit choice behaviour to a large extent. These results evidence that the proposed model framework is able to reproduce the observed exit choice behaviour at the macroscopic and mesoscopic levels.

5.2. Performance comparisons of two pre-evacuation time modelling approaches

5.2.1. Evacuation time

As shown in Fig. 8, compared with the framework using the WD, the framework using the CWM by-and-large obtains the evacuation time curves closer to the observed one. The SC, ERD, EPC and DTET of each scenario are computed and listed in Table 9, and the cases where the metric value of the framework using the CWM is superior over that of the framework using the WD are in bold. It can be clearly seen that the

Table 5
Descriptive statistics of the absolute difference between the simulated and observed average evacuation times of each seat row.

Scenario	Mean (s)		Minimum (s)		Maximum (s)		S.D. (s)	
	CWM	PF	CWM	PF	CWM	PF	CWM	PF
A_FR_MG_N	3.29*	1.94*	0.16	0.34	8.43*	6.87*	2.64*	1.76*
A_F_MG_N	1.06	1.67	0.02	0.29	3.04	3.80	1.05*	1.04*
A_R_MG_N	4.50	5.37	0.13*	0.09*	8.86	11.22	3.10	3.68
B_FRE_ST_D	3.43*	2.62*	0.16*	0.05*	7.35	7.41	2.37*	2.35*
B_FR_ST_D	1.87	2.89	0.06	0.19	5.48*	5.30*	1.84*	1.55*
B_F_ST_D	0.99	1.68	0.11*	0.11*	2.97	4.46	0.88	1.35
B_R_ST_D	4.15	6.83	0.34*	0.00*	15.08	18.63	4.09	6.72
B_E_ST_D	3.34	5.25	0	0.09	13.41*	13.23*	3.77	3.91
B_FR_MA_D	3.41	4.20	0.18	0.19	9.93	11.20	3.15	3.30
B_F_MA_D	2.11	7.04	0.03	0.28	6.73	15.62	2.07	5.00
B_R_MA_D	8.72	10.45	0.69	2.29	15.28	27.56	4.95	8.19
B_FR_MA_N	3.09*	2.43*	0.08	0.10	6.11	7.59	2.35	2.56
B_FR_ST_N	1.94	2.07	0.01	0.05	5.19	5.69	1.64	1.67
Avg. ((CWM-PF)/PF)	-0.145		/		/		/	

Table 6
Results of statistical tests for paired comparisons.

Scenario	Mean (s)		S.D. (s)		*P*-value	
	CWM	PF	CWM	PF	CWM	PF
A_FR_MG_N	1.50	-0.13	4.04	2.68	0.225**	0.866**
A_F_MG_N	-0.78	-0.74	1.29	1.89	0.060**	0.204**
A_R_MG_N	0.46	-4.21	5.62	5.07	0.782**	0.015*
B_FRE_ST_D	-1.74	0.16	3.89	3.60	0.133**	0.876**
B_FR_ST_D	0.19	1.94	2.67	2.71	0.801**	0.024*
B_F_ST_D	0.52	1.10	1.24	1.90	0.152**	0.060**
B_R_ST_D	-2.43	-1.55	5.39	9.65	0.131**	0.573**
B_E_ST_D	-3.13	-1.62	3.96	6.50	0.015*	0.387**
B_FR_MA_D	2.79	3.28	3.76	4.28	0.020*	0.017*
B_F_MA_D	-0.02	7.04	3.02	5.00	0.985**	0.00
B_R_MA_D	2.31	-2.15	10.05	13.43	0.423**	0.574**
B_FR_MA_N	0.55	1.60	3.94	3.18	0.627**	0.094**
B_FR_ST_N	-0.91	0.68	2.43	2.63	0.201**	0.369**

The sign (*) indicates $P > 0.01$, and the sign (**) indicates $P > 0.05$.

framework using the CWM obtains the result closer to the optimal one in 36 out of 52 metric values, and the framework using the WD does not satisfy the validation criteria in one scenario. To make a quantitative performance comparison, Table 10 presents the prediction errors calculated according to the metric values. It shows that in all scenarios except A_FR_MG_N, B_FR_MA_D and B_R_MA_D, the framework using the CWM achieves higher prediction accuracy, with the errors reduced by 25.10 % on average, as compared to the counterpart model.

Moreover, the framework using the WD obtains significantly biased results in simulating the spatial distribution of passenger evacuation times, as presented in Fig. 9. Table 11 shows the statistical parameters of the related simulation errors. It can be found that in the 13 scenarios, the errors from the framework using the CWM are considerably smaller than those from the counterpart model, with a 53.50 % reduction on average.

These results suggest that the inclusion of the dependence of pre-evacuation times on passengers' proximity to the target exit significantly improves the prediction accuracy of the macroscopic and mesoscopic characteristics of passenger evacuation times. In contrast, the evacuation time curves from the framework using the WD are all below those from experiments (see Fig. 8), which implies significantly longer evacuation times. Since the WD randomly generates the pre-evacuation time for each passenger without regard to his/her seat location, those passengers near the exit could be assigned a quite long pre-evacuation time and vice versa. In this way, not only would the evacuation time be substantially prolonged, but the ordered evacuation sequence would also be disrupted. Consequently, the spatial distribution of passenger evacuation times from the framework using the WD exhibits a

Table 7
Results of statistical tests for paired comparisons at the significance level of 5 %.

Time gap type	Paired samples	MWW		K-S		Welch	
		Statistics comparison	H0	Statistics comparison	H0	Statistics comparison	H0
$T_{A\_F\_MG\_N}$	EXP vs. CWM	-3.09<-1.96	Rejected	0.199>0.125	Rejected	1.88<1.97	**Accepted**
	EXP vs. PF	-0.95>-1.96	**Accepted**	0.338>0.125	Rejected	-0.96>-1.97	**Accepted**
$T_{A\_R\_MG\_N}$	EXP vs. CWM	-1.12>-1.96	**Accepted**	0.111<0.116	**Accepted**	-1.64>-1.97	**Accepted**
	EXP vs. PF	-9.12<-1.96	Rejected	0.554>0.115	Rejected	4.69>1.97	Rejected
$T_{B\_F\_ST\_D}$	EXP vs. CWM	-0.25>-1.96	**Accepted**	0.150>0.117	Rejected	0.29<1.97	**Accepted**
	EXP vs. PF	-1.00>-1.96	**Accepted**	0.230>0.118	Rejected	-1.66>-1.97	**Accepted**
$T_{B\_R\_ST\_D}$	EXP vs. CWM	-1.00>-1.96	**Accepted**	0.128>0.104	Rejected	0.33<1.96	**Accepted**
	EXP vs. PF	-1.70>-1.96	**Accepted**	0.286>0.105	Rejected	-0.09>-1.97	**Accepted**
$T_{B\_E\_ST\_D}$	EXP vs. CWM	-1.58>-1.96	**Accepted**	0.290>0.137	Rejected	-0.08>-1.97	**Accepted**
	EXP vs. PF	-0.23>-1.96	**Accepted**	0.112<0.137	**Accepted**	-1.10>-1.97	**Accepted**
$T_{B\_F\_MA\_D}$	EXP vs. CWM	-0.50>-1.96	**Accepted**	0.099<0.125	**Accepted**	1.39<1.97	**Accepted**
	EXP vs. PF	-6.74<-1.96	Rejected	0.434>0.125	Rejected	-6.79<-1.97	Rejected
$T_{B\_R\_MA\_D}$	EXP vs. CWM	-2.93<-1.96	Rejected	0.178>0.120	Rejected	-1.63>-1.97	**Accepted**
	EXP vs. PF	-3.76<-1.96	Rejected	0.385>0.120	Rejected	-2.48<-1.97	Rejected
$T_{B\_F\_ST\_N}$	EXP vs. CWM	-0.88>-1.96	**Accepted**	0.151<0.185	**Accepted**	0.47<2.00	**Accepted**
	EXP vs. PF	-0.30>-1.96	**Accepted**	0.243>0.186	Rejected	-2.04<-2.00	Rejected
$T_{B\_R\_ST\_N}$	EXP vs. CWM	-0.30>-1.96	**Accepted**	0.162>0.158	Rejected	1.75<2.00	**Accepted**
	EXP vs. PF	-0.77>-1.96	**Accepted**	0.240>0.157	Rejected	1.21<1.99	**Accepted**
$T_{B\_F\_MA\_N}$	EXP vs. CWM	-0.23>-1.96	**Accepted**	0.083<0.180	**Accepted**	-0.12>-1.99	**Accepted**
	EXP vs. PF	-3.49<-1.96	Rejected	0.451>0.179	Rejected	-3.58<-1.99	Rejected
$T_{B\_R\_MA\_N}$	EXP vs. CWM	-0.83>-1.96	**Accepted**	0.146<0.163	**Accepted**	0.62<1.98	**Accepted**
	EXP vs. PF	-0.39>-1.96	**Accepted**	0.212>0.161	Rejected	-0.69>-1.99	**Accepted**

Table 8
Results of statistical tests for paired comparisons at the significance level of 5 %.

Flow type	Paired samples	MWW		K-S		Welch	
		Statistics comparison	H0	Statistics comparison	H0	Statistics comparison	H0
$F_{A\_FR\_MG\_N}$	EXP vs. CWM	-2.21<-1.96	Rejected	0.172>0.112	Rejected	2.49>1.96	Rejected
	EXP vs. PF	-0.86>-1.96	**Accepted**	0.135>0.110	Rejected	0.920<1.97	**Accepted**
$F_{A\_F\_MG\_N}$	EXP vs. CWM	-3.06<-1.96	Rejected	0.199>0.125	Rejected	-1.87>-1.97	**Accepted**
	EXP vs. PF	-0.77>-1.96	**Accepted**	0.269>0.125	Rejected	-1.22>-1.97	**Accepted**
$F_{A\_R\_MG\_N}$	EXP vs. CWM	-1.12>-1.96	**Accepted**	0.111<0.116	**Accepted**	2.12>1.97	Rejected
	EXP vs. PF	-9.07<-1.96	Rejected	0.554>0.115	Rejected	-7.92<-1.97	Rejected
$F_{B\_F\_ST\_D}$	EXP vs. CWM	-0.97>-1.96	**Accepted**	0.145>0.117	Rejected	-0.48>-1.97	**Accepted**
	EXP vs. PF	-0.50>-1.96	**Accepted**	0.230>0.118	Rejected	-0.49>-1.97	**Accepted**
$F_{B\_R\_ST\_D}$	EXP vs. CWM	-0.47>-1.96	**Accepted**	0.121>0.105	Rejected	1.17<1.96	**Accepted**
	EXP vs. PF	-1.34>-1.96	**Accepted**	0.241>0.105	Rejected	-2.05<-1.97	Rejected
$F_{B\_E\_ST\_D}$	EXP vs. CWM	-1.94>-1.96	**Accepted**	0.290>0.137	Rejected	-2.41<-1.97	Rejected
	EXP vs. PF	-0.12>-1.96	**Accepted**	0.112<0.137	**Accepted**	1.39<1.97	**Accepted**
$F_{B\_F\_MA\_D}$	EXP vs. CWM	-0.61>-1.96	**Accepted**	0.100<0.125	**Accepted**	-0.31>-1.97	**Accepted**
	EXP vs. PF	-6.57<-1.96	Rejected	0.557>0.200	Rejected	-5.54<-2.00	Rejected
$F_{B\_R\_MA\_D}$	EXP vs. CWM	-2.90<-1.96	Rejected	0.198>0.120	Rejected	4.08>1.97	Rejected
	EXP vs. PF	-3.89<-1.96	Rejected	0.385>0.120	Rejected	-4.50<-1.97	Rejected
$F_{B\_FR\_ST\_D}$	EXP vs. CWM	-0.17>-1.96	**Accepted**	0.079<0.157	**Accepted**	-0.31>-1.98	**Accepted**
	EXP vs. PF	-1.72>-1.96	**Accepted**	0.145<0.157	**Accepted**	2.80>1.99	Rejected
$F_{B\_FRE\_ST\_D}$	EXP vs. CWM	-0.28>-1.96	**Accepted**	0.121<0.155	**Accepted**	0.28<1.98	**Accepted**
	EXP vs. PF	-1.66>-1.96	**Accepted**	0.160>0.155	Rejected	1.84<1.98	**Accepted**
$F_{B\_FR\_MA\_D}$	EXP vs. CWM	-2.66<-1.96	Rejected	0.198>0.159	Rejected	3.54>1.98	Rejected
	EXP vs. PF	-1.17>-1.96	**Accepted**	0.189>0.159	Rejected	3.88>1.99	Rejected
$F_{B\_F\_ST\_N}$	EXP vs. CWM	-0.95>-1.96	**Accepted**	0.151<0.185	**Accepted**	-0.48>-2.00	**Accepted**
	EXP vs. PF	-0.34>-1.96	**Accepted**	0.236>0.186	Rejected	0.56<2.00	**Accepted**
$F_{B\_R\_ST\_N}$	EXP vs. CWM	-0.4>-1.96	**Accepted**	0.160>0.158	Rejected	-0.05>-1.98	**Accepted**
	EXP vs. PF	-0.76>-1.96	**Accepted**	0.227>0.157	Rejected	-1.26>-1.99	**Accepted**
$F_{B\_FR\_ST\_N}$	EXP vs. CWM	-0.66>-1.96	**Accepted**	0.130<0.139	**Accepted**	0.54<1.97	**Accepted**
	EXP vs. PF	-0.20>-1.96	**Accepted**	0.090<0.139	**Accepted**	0.31<1.97	**Accepted**
$F_{B\_F\_MA\_N}$	EXP vs. CWM	-0.14>-1.96	**Accepted**	0.083<0.180	**Accepted**	0.50<1.99	**Accepted**
	EXP vs. PF	-3.55<-1.96	Rejected	0.451>0.179	Rejected	2.31>1.99	Rejected
$F_{B\_R\_MA\_N}$	EXP vs. CWM	-0.79>-1.96	**Accepted**	0.146<0.165	**Accepted**	0.92<1.98	**Accepted**
	EXP vs. PF	-0.39>-1.96	**Accepted**	0.212>0.161	Rejected	-0.34>-1.99	**Accepted**
$F_{B\_FR\_MA\_N}$	EXP vs. CWM	-1.34>-1.96	**Accepted**	0.204>0.140	Rejected	0.35<1.98	**Accepted**
	EXP vs. PF	-0.61>-1.96	**Accepted**	0.107<0.140	**Accepted**	0.40<1.97	**Accepted**

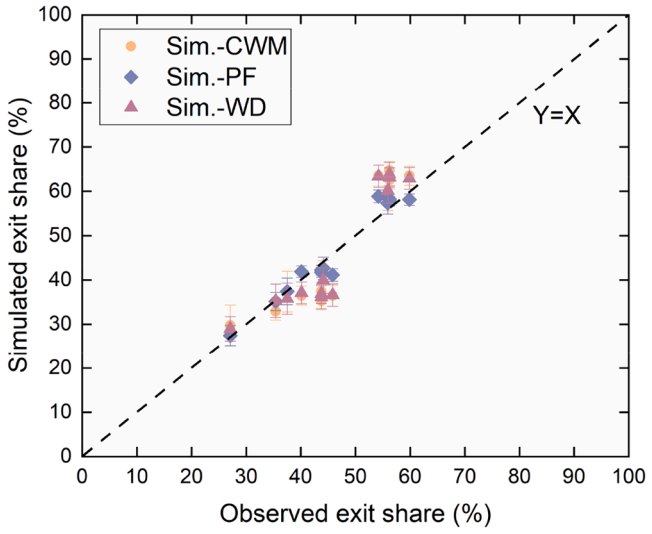

Fig. 10. Simulated and observed exit shares.

permanently weaker dependence on the seat row number than that from experiments (see Fig. 9).

5.2.2. Alighting time gap

As illustrated in Table C.1 (see Supplementary material C), for all alighting time gap samples except $T_{A\_R\_MG\_N}$, the mean value from the framework using the WD is larger than that from experiments. This is consistent with the aforementioned observations and should be attributed to the prolonged evacuation time. Three non-parametric hypothesis tests are conducted to statistically examine the degree of match between the alighting time gap samples from experiments and the framework using the WD, shown in Table 12. The results in Tables 7 and 12 indicate that much more acceptance results of the null hypothesis and alighting time gap samples that accept the null hypothesis are observed in the framework using the CWM than in the framework using the WD (25 vs. 17 and 11 vs. 8). This suggests that the use of the CWM facilitates higher prediction accuracy of the passenger alighting time gap distribution characteristics as compared to using the WD, with a 25.76 % improvement on average.

5.2.3. Flow rate

Table 13 presents the results of the three non-parametric hypothesis tests related to the framework using the WD. As shown in Tables 8 and 13, though the framework using the WD obtains slightly more flow samples (15 vs. 14) that accept the null hypothesis in at least one test than the framework using the CWM, more acceptance results of the null hypothesis are observed for the latter (31 vs. 33). In accordance with the results related to alighting time gaps, the framework using the CWM presents higher prediction accuracy in single-exit scenarios. As the increased number of available exits is beneficial to alleviate the delayed effect induced by using the WD, the obtained prediction accuracy is even slightly higher in multi-exit scenarios. Thus, the frameworks using the CWM and the WD generally exhibit a comparable accuracy performance in predicting the instantaneous flow rate distribution characteristics of passengers.

5.2.4. Exit choice

As for the exit choices, there is no prominent difference between the results from the frameworks using the CWM and the WD, illustrated in Figs. 10 and 11. These results suggest that using two different pre-

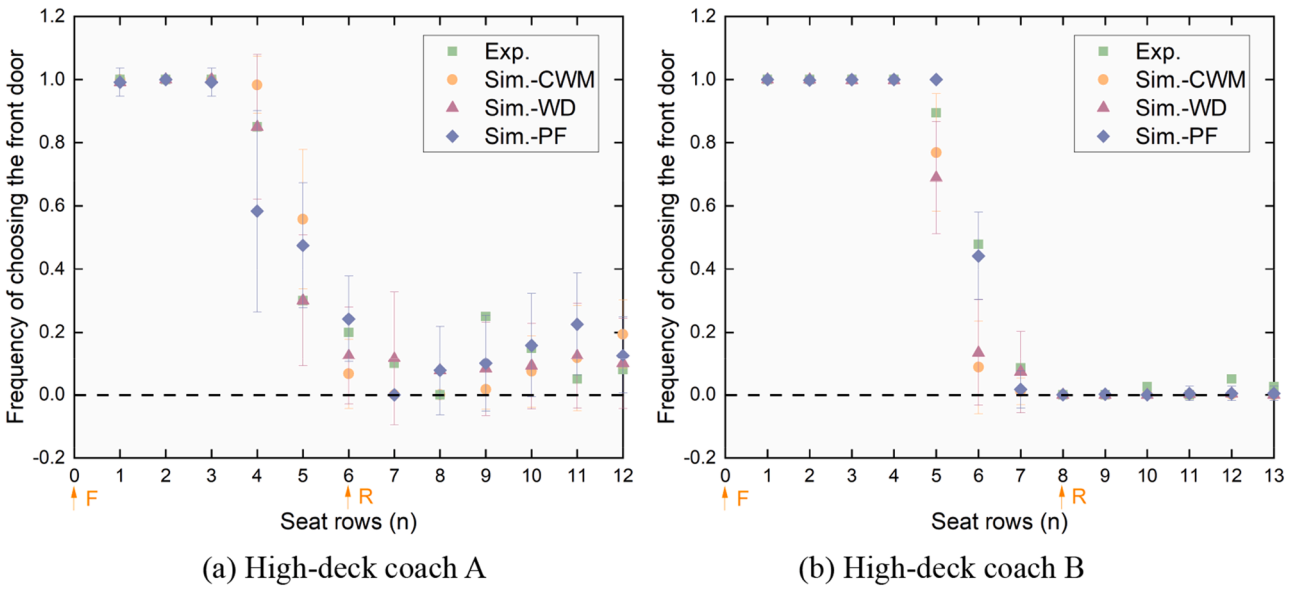

Fig. 11. Spatial distribution of passenger exit choices from simulations and experiments. The orange arrows F and R indicate the positions of the front and rear doors, respectively. And, the frequency of '0' and '1' means that all passengers choose the rear door and the front door, respectively.

Table 9
Validation metric values related to the evacuation time curve for the frameworks using the CWM and the WD, where the symbol indicates whether the validation criteria are satisfied ($\surd$ = satisfied, and $\times$ = not satisfied).

Scenario	SC		ERD		EPC		DTET		Satisfaction	
	CWM	WD	CWM	WD	CWM	WD	CWM	WD	CWM	WD
A_FR_MG_N	**0.950**	**0.924**	0.098	0.060	1.106	0.972	0.084	0.001	$\surd$	$\surd$
A_F_MG_N	**0.958**	**0.954**	**0.029**	**0.177**	**0.990**	**0.850**	**0.020**	**0.160**	$\surd$	$\surd$
A_R_MG_N	0.927	0.927	**0.031**	**0.052**	**0.989**	**0.957**	0.016	0.001	$\surd$	$\surd$
B_FRE_ST_D	**0.854**	**0.810**	**0.038**	**0.359**	**1.010**	**0.744**	**0.032**	**0.240**	$\surd$	$\times$
B_FR_ST_D	0.935	0.936	**0.046**	**0.131**	**1.010**	**0.898**	0.065	0.011	$\surd$	$\surd$
B_F_ST_D	0.979	0.979	**0.031**	**0.118**	**0.974**	**0.896**	**0.031**	**0.106**	$\surd$	$\surd$
B_R_ST_D	**0.966**	**0.960**	**0.075**	**0.146**	**0.935**	**0.875**	**0.043**	**0.100**	$\surd$	$\surd$
B_E_ST_D	**0.972**	**0.938**	**0.076**	**0.142**	**0.944**	**0.892**	**0.018**	**0.055**	$\surd$	$\surd$
B_FR_MA_D	**0.922**	**0.907**	0.118	0.045	1.128	1.039	0.114	0.056	$\surd$	$\surd$
B_F_MA_D	**0.973**	**0.964**	**0.018**	**0.051**	**0.990**	**0.953**	**0.010**	**0.042**	$\surd$	$\surd$
B_R_MA_D	0.965	0.965	0.061	0.060	1.047	0.956	0.068	0.016	$\surd$	$\surd$
B_FR_MA_N	**0.899**	**0.868**	**0.034**	**0.112**	**1.001**	**0.912**	0.065	0.024	$\surd$	$\surd$
B_FR_ST_N	**0.952**	**0.944**	**0.051**	**0.135**	**0.963**	**0.886**	**0.011**	**0.059**	$\surd$	$\surd$

Table 10
Performance comparisons between the frameworks using the CWM and the WD based on the prediction error from the four metrics related to the evacuation time curve.

Scenario	CWM	WD	Ratio=(CWM-WD)/WD
A_FR_MG_N	0.338	0.165	**1.048***
A_F_MG_N	0.101	0.533	**-0.811**
A_R_MG_N	0.131	0.169	**-0.225**
B_FRE_ST_D	0.226	1.045	**-0.784**
B_FR_ST_D	0.186	0.308	**-0.396**
B_F_ST_D	0.109	0.349	**-0.688**
B_R_ST_D	0.217	0.411	**-0.472**
B_E_ST_D	0.178	0.367	**-0.515**
B_FR_MA_D	0.438	0.233	**0.880***
B_F_MA_D	0.065	0.176	**-0.631**
B_R_MA_D	0.211	0.155	**0.361***
B_FR_MA_N	0.201	0.356	**-0.435**
B_FR_ST_N	0.147	0.364	**-0.596**
	Avg.		**-0.251**

For each scenario, the error value in Table 10 is defined as the sum of the prediction error (|simulated value − optimal value|) of each metric.

evacuation time modelling approaches has no significant impact on the prediction accuracy of passenger exit choices at the macroscope and mesoscopic levels.

5.3. *Effects of overtaking behaviour*

As shown in Fig. C.1 (see Supplementary material C), a higher proportion of radical passengers (P_N^r) leads to a greater number of overtaking behaviour, which justifies the developed behavioural rules. More detailed results are illustrated in the ensuing sections.

5.3.1. *Evacuation time*

In relation to evacuation efficiency, a significant negative effect of overtaking behaviour is observed, shown in Fig. 12(a) and (b). As the proportion of radical passengers increases, the evacuation times become longer and the evacuation time curve exhibits a more significant non-monotonic characteristic. The survival functions of the alighting time gap with different proportions of radical passengers are also presented in Fig. C.2 (see Supplementary material C). It can be clearly seen that the higher the proportion of radical passengers is, the greater the probability is for a longer alighting time gap, which means longer clogs. These results suggest that the lower evacuation efficiency resulting from

Table 11
Descriptive statistics of the absolute difference between the simulated and observed average evacuation times of each seat row.

Scenario	Mean (s)		Minimum (s)		Maximum (s)		S.D. (s)	
	WD	CWM- WD	WD	CWM- WD	WD	CWM- WD	WD	CWM- WD
A_FR_MG_N	3.98	-0.69	0.27	-0.11	9.49	-1.06	3.23	-0.59
A_F_MG_N	6.23	-5.17	1.12	-1.10	12.83	-9.79	4.09	-3.04
A_R_MG_N	11.74	-7.24	1.21	-1.08	24.31	-15.45	7.86	-4.76
B_FRE_ST_D	8.83	-5.4	2.37	-2.21	18.91	-11.56	4.90	-2.53
B_FR_ST_D	5.41	-3.54	0.81	-0.75	11.26	-5.78	3.17	-1.33
B_F_ST_D	4.02	-3.03	0.11	0	8.00	-5.03	2.51	-1.63
B_R_ST_D	8.35	-4.20	0.74	-0.40	19.03	-3.95	5.01	-0.92
B_E_ST_D	11.21	-7.87	0.36	-0.36	25.74	-12.33	8.18	-4.41
B_FR_MA_D	6.05	-2.64	1.28	-1.10	11.97	-2.04	3.35	-0.20
B_F_MA_D	3.87	-1.76	0.22	-0.19	8.74	-2.01	2.66	-0.59
B_R_MA_D	11.50	-2.78	1.70	-1.01	25.25	-9.97	7.62	-2.67
B_FR_MA_N	4.63	-1.54	0.94	-0.86	12.48	-6.37	3.73	-1.38
B_FR_ST_N	5.52	-3.58	1.03	-1.02	11.94	-6.75	3.88	-2.24
Avg. ((CWM-WD)/WD)	-0.535		/		/		/	

Table 12
Results of statistical tests for paired comparisons at the significance level of 5 %.

Time gap type	Paired samples	MWW		K-S		Welch	
		Statistics comparison	H0	Statistics comparison	H0	Statistics comparison	H0
$T_{A\_F\_MG\_N}$	EXP vs. WD	-5.02<-1.96	Rejected	0.262>0.125	Rejected	4.65>1.97	Rejected
$T_{A\_R\_MG\_N}$	EXP vs. WD	-1.36>-1.96	**Accepted**	0.119>0.116	Rejected	-1.78>-1.97	**Accepted**
$T_{B\_F\_ST\_D}$	EXP vs. WD	-2.00<-1.96	Rejected	0.165>0.118	Rejected	3.63>1.97	Rejected
$T_{B\_R\_ST\_D}$	EXP vs. WD	-0.30>-1.96	**Accepted**	0.110>0.105	Rejected	2.79>1.97	Rejected
$T_{B\_E\_ST\_D}$	EXP vs. WD	-1.64>-1.96	**Accepted**	0.277>0.136	Rejected	0.21<1.98	**Accepted**
$T_{B\_F\_MA\_D}$	EXP vs. WD	-0.63>-1.96	**Accepted**	0.088<0.125	**Accepted**	1.34<1.97	**Accepted**
$T_{B\_R\_MA\_D}$	EXP vs. WD	-1.27>-1.96	**Accepted**	0.150>0.120	Rejected	1.18<1.97	**Accepted**
$T_{B\_F\_ST\_N}$	EXP vs. WD	-1.09>-1.96	**Accepted**	0.169<0.185	**Accepted**	0.35<2.00	**Accepted**
$T_{B\_R\_ST\_N}$	EXP vs. WD	-1.23>-1.96	**Accepted**	0.197>0.158	Rejected	3.61>2.0	Rejected
$T_{B\_F\_MA\_N}$	EXP vs. WD	-2.55<-1.96	Rejected	0.232>0.180	Rejected	3.43>1.99	Rejected
$T_{B\_R\_MA\_N}$	EXP vs. WD	-0.35>1.96	**Accepted**	0.144<0.163	**Accepted**	1.77<1.98	**Accepted**

Table 13
Results of statistical tests for paired comparisons at the significance level of 5 %.

Flow type	Paired samples	MWW		K-S		Welch	
		Statistics comparison	H0	Statistics comparison	H0	Statistics comparison	H0
$F_{A\_FR\_MG\_N}$	EXP vs. WD	-0.97>-1.96	**Accepted**	0.133>0.111	Rejected	1.73<1.96	**Accepted**
$F_{A\_F\_MG\_N}$	EXP vs. WD	-5.02<-1.96	Rejected	0.262>1.25	Rejected	-4.40<-1.97	Rejected
$F_{A\_R\_MG\_N}$	EXP vs. WD	-1.36>-1.96	**Accepted**	0.119>0.116	Rejected	2.40>1.97	Rejected
$F_{B\_F\_ST\_D}$	EXP vs. WD	-2.00<-1.96	Rejected	0.165>0.117	Rejected	-1.94>-1.97	**Accepted**
$F_{B\_R\_ST\_D}$	EXP vs. WD	-0.66>-1.96	**Accepted**	0.126>0.105	Rejected	-0.31>-1.96	**Accepted**
$F_{B\_E\_ST\_D}$	EXP vs. WD	-1.89>-1.96	**Accepted**	0.277>0.136	Rejected	-2.54<-1.98	Rejected
$F_{B\_F\_MA\_D}$	EXP vs. WD	-0.86>-1.96	**Accepted**	0.090<0.126	**Accepted**	-0.62>-1.97	**Accepted**
$F_{B\_R\_MA\_D}$	EXP vs. WD	-1.26>-1.96	**Accepted**	0.175>0.120	Rejected	2.34>1.97	Rejected
$F_{B\_FR\_ST\_D}$	EXP vs. WD	-0.38>-1.96	**Accepted**	0.071<0.157	**Accepted**	-0.61>-1.98	**Accepted**
$F_{B\_FRE\_ST\_D}$	EXP vs. WD	-0.67>-1.96	**Accepted**	0.121<0.155	**Accepted**	-0.30>-1.98	**Accepted**
$F_{B\_FR\_MA\_D}$	EXP vs. WD	-1.88>-1.96	**Accepted**	0.196>0.159	Rejected	2.84>1.98	Rejected
$F_{B\_F\_ST\_N}$	EXP vs. WD	-1.09>-1.96	**Accepted**	0.169<0.185	**Accepted**	-0.36>-2.00	**Accepted**
$F_{B\_R\_ST\_N}$	EXP vs. WD	-1.28>-1.96	**Accepted**	0.197>0.158	Rejected	-1.20>-1.98	**Accepted**
$F_{B\_FR\_ST\_N}$	EXP vs. WD	-0.33>-1.96	**Accepted**	0.128<0.139	**Accepted**	-0.21>-1.98	**Accepted**
$F_{B\_F\_MA\_N}$	EXP vs. WD	-2.65<-1.96	Rejected	0.232>0.180	Rejected	-2.40<-1.99	Rejected
$F_{B\_R\_MA\_N}$	EXP vs. WD	-0.38>-1.96	**Accepted**	0.144<0.165	**Accepted**	-0.21>-1.98	**Accepted**
$F_{B\_FR\_MA\_N}$	EXP vs. WD	-1.26>-1.96	**Accepted**	0.205>0.140	Rejected	0.85<1.98	**Accepted**

overtaking behaviour could be ascribed to the induced more serious congestion within the narrow aisle [23,25], which leads to longer clogs and thus reduces the outflow (also demonstrated by Figs. 13(b) and 14). Such a negative effect gradually saturates when the proportion of radical passengers increases to exceed a certain value (i.e., 75 %). Nevertheless, these results suggest that high-deck coach passengers never benefit from any overtaking behaviour, which provides consistent evidence with two previous studies [23,25] as to the negative effect of overtaking behaviour, but is different from the results in [24] who observed its invariably positive effect in unidirectional flows. It should be noted that aside from the unidirectional flow [24], all the other three scenarios (i.e., an aircraft [23], a room [25] and a high-deck coach) involve the narrow bottleneck, which is recognised as the critical structural element that triggers off serious crowd congestion [28]. In such scenarios, though overtaking behaviour facilitates higher movement velocity for occupants, the induced crowd congestion after the exit capacity is saturated would conversely reduce the evacuation efficiency, i.e., the "faster is slower" effect [25,28]. Moreover, since the exit capacity of high-deck coaches is rather limited due to the quite narrow aisle and exit, overtaking behaviour does not induce any benefit to passengers. This

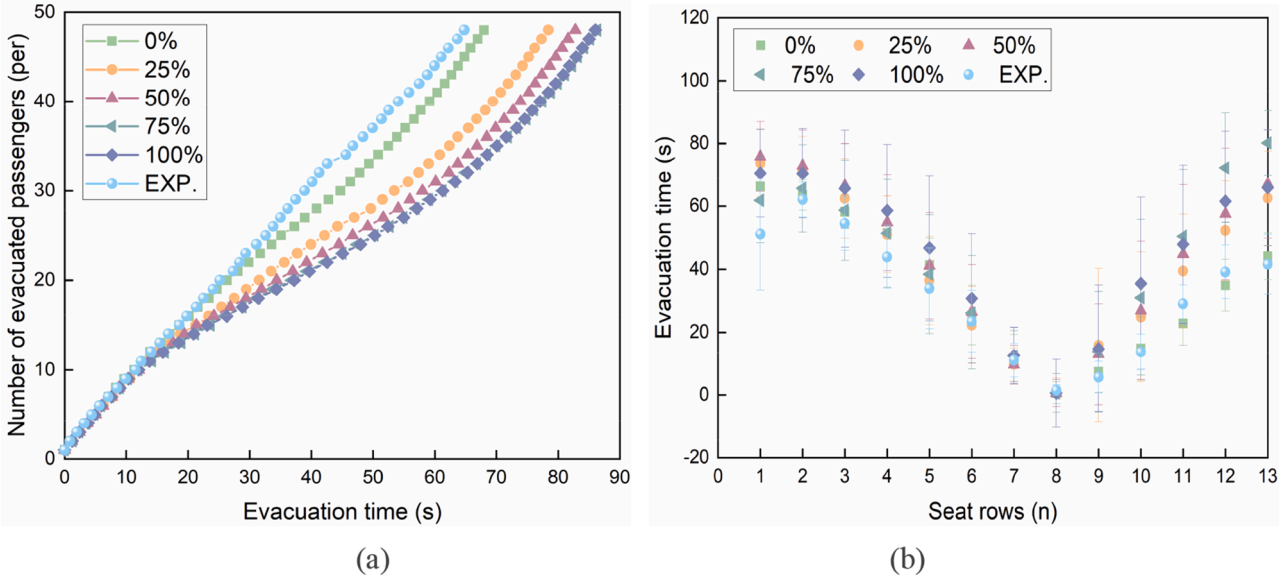

Fig. 12. Effects of overtaking behaviour on the evacuation time in scenario B_R_ST_D. Plots (a) and (b) respectively show the evacuation time curves and the spatial distribution of passenger evacuation times.

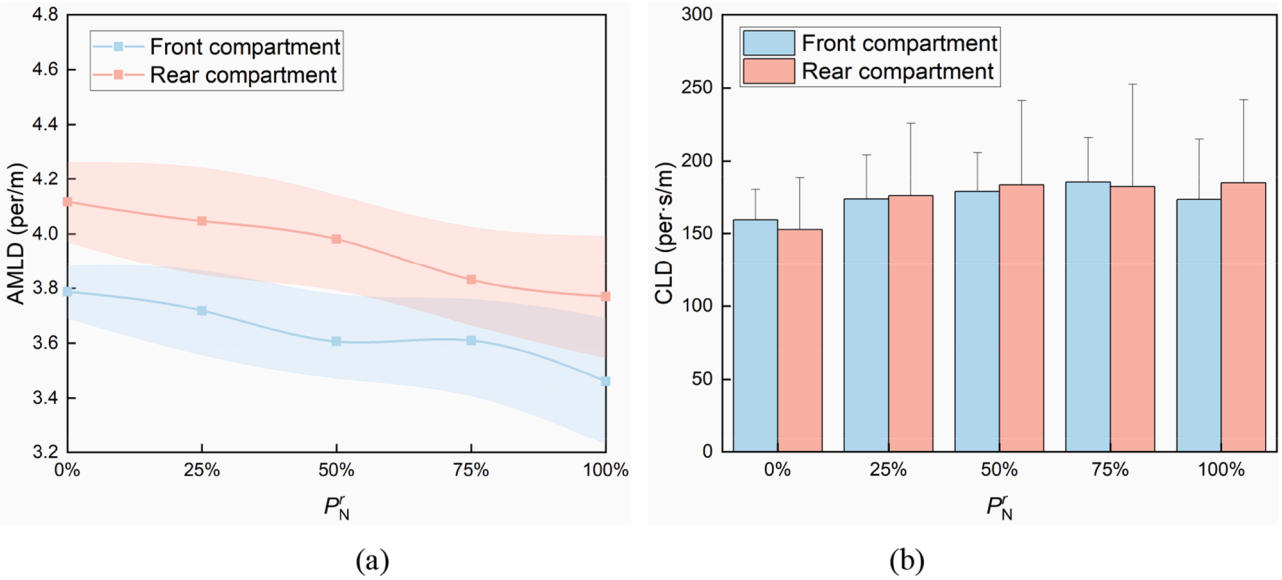

Fig. 13. Effects of overtaking behaviour on the average maximum linear density (AMLD, plot (a)) and the cumulative linear density (CLD, plot (b)) within the aisle in scenario B_R_ST_D.

highlights the peculiarity of high-deck coach evacuation scenarios.

5.3.2. *Crowdedness*

Fig. 13 presents the sensitivity of the AMLD and CLD to P_N^r. A greater number of overtaking behaviour requires more frequent changes of the passenger body posture, which in turn leads to more empty cells within the aisle and thus reduces its maximum passenger capacity, i.e., AMLD (see Fig. 13(a)). However, this does not mean a decrease in the level of crowdedness. Conversely, overtaking behaviour would significantly increase the duration of congestion (see Fig. 12) and thus result in increasing CLD (see Fig. 13(b)), which is the more comprehensive metric for measuring crowdedness [1]. A higher level of crowdedness implies a greater evacuation risk. Thus, these results suggest that any overtaking behaviour is detrimental to the evacuation safety of the overall passenger system.

To further unmask the potential reasons for these phenomena, Fig. 14 shows the DD of passengers, with P_N^r varying from 0 to 1. It can be clearly seen that an ordered passenger queue within the aisle dissolves and gradually transitions to a disordered state as the number of overtaking behaviour increases. In this process, overtaking behaviour enables passengers at the end of the queue to move forwards and thus mitigates the queuing phenomenon and local congestion. On the other hand, the overtaking passengers induce more serious congestion near the merging area before the stairway. Moreover, the aisle in the rear compartment gradually becomes more congested than that of the front compartment. This could be ascribed to the higher passenger capacity in the rear compartment (5.62 per/m vs. 5.15 per/m), leading to significantly more potential conflicts. These results suggest that overtaking behaviour could be conducive to those passengers far away from the exits, but this is at the expense of overall evacuation efficiency and safety.

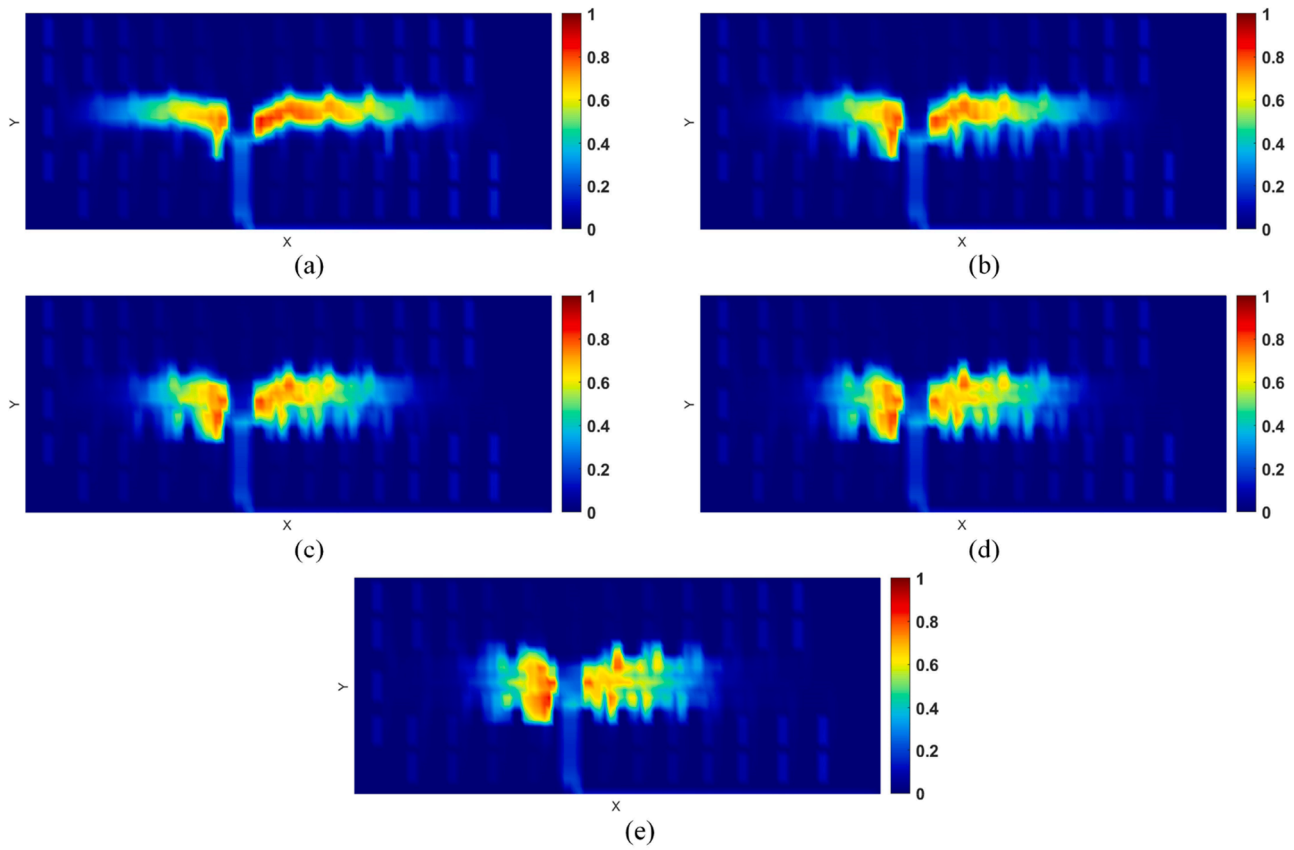

Fig. 14. Density distribution (DD) map in scenario B_R_ST_D. In plots (a)-(e), P_N^r is set as 0, 25 %, 50 %, 75 % and 100 % respectively.

6. Conclusions

While guaranteeing safety in evacuation from a high-deck coach presents serious challenges, a dedicated high-deck coach evacuation model is absent, let alone exploratory simulation analyses. To fill these gaps, a high-deck coach evacuation model framework comprised of the strategic, tactical and operational behavioural modules is proposed for the first time. In the strategic behaviour module, the CWM is deployed to capture the pre-evacuation times of passengers so that both the distribution characteristics and the dependence on the proximity to the target exit are encapsulated. In the tactical and operational behaviour modules, elaborate behavioural rules are developed and coupled with CPT to comprehensively incorporate the typical behavioural characteristics and decision-making factors in high-deck coach evacuations (e.g., overtaking). The framework is validated across various high-deck coach evacuation scenarios, demonstrating its universality. Moreover, systematic simulation analyses are conducted to explore the efficacy of two widely used pre-evacuation time modelling methods from the perspective of system simulation accuracy and the effects of overtaking behaviour on high-deck coach evacuations.

The simulation results related to the evacuation times, flow rates, alighting time gaps and exit choices from the proposed framework accord closely with those from experiments, demonstrating its capability to replicate high-deck coach passenger evacuation behaviours. Compared with the Pathfinder model - the state-of-the-art passenger evacuation model, the proposed framework produces the results closer to experimental data regarding evacuation times, flow rates and alighting time gaps, with respectively 13.20 %, 34.85 % and 8.82 % performance improvements on average, while achieving comparable accuracy in predicting the exit choice behaviour. Comparative analyses indicate that the use of the CWM substantially improves the prediction accuracy of the evacuation times and alighting time gaps as compared to using the WD, with the errors respectively reduced by 39.30 % and 25.76 % on average. These results imply the importance of considering the effect of proximity to the target exit in the pre-evacuation time modelling, especially for those venues with dense seat rows and narrow aisles. Furthermore, simulation analyses indicate that overtaking behaviour has significant effects on high-deck coach evacuation efficiency and crowdedness, but does not induce any benefit for the overall passenger system. These findings suggest that effective training and guidelines should be developed to help passengers avoid such aggressive behaviour.

The validation results not only demonstrate the effectiveness of the proposed framework, but also confirm the applicability and generalizability of the parameter values used. Thus, our framework can serve as an effective tool to predict high-deck coach passenger evacuations, making it possible to evaluate and optimise high-deck coach evacuation performance in various environments, as well as develop useful design guidelines.

In future work, there are several promising research lines that warrant further attention. First, the proposed framework should be further extended to incorporate more typical behavioural characteristics (e.g., group behaviour), which would be helpful to further improve its prediction accuracy and applicability. Second, exploring a multi-scale modelling theory that can effectively balance computation efficiency and spatial discretisation would be a promising topic from the perspective of engineering. Third, further investigation is warranted to examine the performance advantage of the CWM in other scenarios such as high-rise buildings. Moreover, dedicated simulation analyses should be conducted to develop effective behaviour and layout optimisation strategies (e.g., aisle width adjustments) to enhance the evacuation performance. To tackle these challenges, the development of specific rules, algorithms and strategies may be necessary.

CRediT authorship contribution statement

Rong Huang: Writing – original draft, Methodology, Funding acquisition, Conceptualization. **Xuan Zhao:** Validation, Resources, Formal analysis, Conceptualization. **Yuzhou Yang:** Validation, Software, Investigation, Data curation. **Qingshan Liu:** Visualization, Validation, Software, Funding acquisition. **Yufei Yuan:** Writing – original draft, Supervision, Methodology, Investigation. **Winnie Daamen:** Writing – original draft, Validation, Supervision.

Declaration of competing interest

The authors declare that they have no known competing financial interests or personal relationships that could have appeared to influence the work reported in this paper.

Acknowledgements

This work was supported by the Postdoctoral Fellowship Program of CPSF (GZC20241449 and GZC20241445), Natural Science Basic Research Program of Shaanxi (2025JC-YBQN-474), Shaanxi Provincial International Joint Research Centre for Key Technologies of Vehicle Intelligence and Electrification (2025GH-GHJD-028), and the Fundamental Research Funds for the Central Universities (CHD, 300102224102).

Supplementary materials

Supplementary material associated with this article can be found, in the online version, at doi:10.1016/j.ress.2025.111582.

Data availability

Data will be made available on request.

References

[1] Huang R, Zhao X, Yuan Y, Yu Q, Zhou C, Daamen W. Experimental study on evacuation behaviour of passengers in a high-deck coach: a Chinese case study. Phys A: Stat Mech Appl 2021;579:126120.
[2] Junfeng C, Maohua Z, Peiyun Q, Zeng L, Jiacheng C. Mapping the fire risk in buildings: a hybrid method of ASET-RSET concept and FED concept. Reliab Eng Syst Saf 2023;240:109571.
[3] He Z, Shen K, Lan M, Weng W. The effects of dynamic multi-hazard risk assessment on evacuation strategies in chemical accidents. Reliab Eng Syst Saf 2024;246:110044.
[4] Luan T, Gai W, Sun D, Dong H. Emergency evacuation risk assessment for toxic gas attacks in airport terminals: model, algorithm, and application. Reliab Eng Syst Saf 2025;253:110576.
[5] Ding Z, Xu S, Xie X, Zheng K, Wang D, Fan J, Li H, Liao L. A building information modeling-based fire emergency evacuation simulation system for large infrastructures. Reliab Eng Syst Saf 2024;244:109917.
[6] Peng J, Wei Z, Chen Y, Wang S, Li Y, Wang S, Taku F. Heterogeneous pedestrian simulation in commercial complexes: when attractive potential meets social force. IEEE Trans Intell Transp Syst 2025:1–18.
[7] Huang R, Zhao X, Yuan Y, Yu Q, Daamen W. Open experimental data-sets to reveal behavioural insights of high-deck coach evacuations. Fire Technol 2022.
[8] Huang R, Zhao X, Yuan Y, Yu Q, Liu C, Daamen W. Modeling pedestrian tactical and operational decisions under risk and uncertainty: a two-layer model framework. IEEE Trans Intell Transp Syst 2023;24:5259–81.
[9] Galea ER, Blake SJ, Lawrence PJ. Report on the testing and systematic evaluation of the airEXODUS aircraft evacuation model. In: Civil aviation authority (CAA); 2005.
[10] Alonso V, Abreu OV, Cuesta A, Silió D. A new approach for modelling passenger trains evacuation procedures. Procedia - Soc Behav Sci 2014;160:284–93.
[11] Galea ER, Deere S, Brown R, Filippidis L. An experimental validation of an evacuation model using data sets generated from two large passenger ships. J. Sh Res 2013:57.
[12] Li Z, Xu C, Bian Z. A force-driven model for passenger evacuation in bus fires. Phys A: Stat Mech Appl 2021:126591.
[13] Huang S. Study of pedestrian movement characteristics and evacuation behaviors in seat aisle area of high-speed train. Hefei: University of Science and Technology of China; 2019.
[14] Haghani M, Sarvi M. Stated and revealed exit choices of pedestrian crowd evacuees. Transp Res B: Methodol 2017;95:238–59.
[15] Lu P, Li Y. Agent-based fire evacuation model using social learning theory and intelligent optimization algorithms. Reliab Eng Syst Saf 2025;260:111000.
[16] Kim G, Heo G. Agent-based radiological emergency evacuation simulation modeling considering mitigation infrastructures. Reliab Eng Syst Saf 2023;233:109098.
[17] Li Y, Xiao Q, Gu J, Cai W, Hu M. Modeling and solving Passenger ship evacuation arrangement problem. Reliab Eng Syst Saf 2024;246:110075.
[18] Yang Y, Xie D-F, Zhao X-M, Jia B. Two-stage stochastic optimization of passenger evacuation routes in metro stations considering stampede incidents. Reliab Eng Syst Saf 2025;260:111047.
[19] Yang X, Dai W, Li Y, Yang X. An efficient evacuation path optimization for passengers in subway stations under floods. Tunn Undergr Space Technol 2024;143:105473.
[20] Haghani M, Sarvi M, Scanlon L. Simulating pre-evacuation times using hazard-based duration models: is waiting strategy more efficient than instant response? Saf Sci 2019;117:339–51.
[21] Haghani M, Sarvi M. Crowd model calibration at strategic, tactical, and operational levels: full-spectrum sensitivity analyses show bottleneck parameters are most critical, followed by exit-choice-changing parameters. Transp Lett 2024;16:354–81.
[22] Galea ER, Deere SJ, Hopkin CG, Xie H. Evacuation response behaviour of occupants in a large theatre during a live performance. Fire Mater 2017;41:467–92.
[23] Song C, Shao Q, Zhu P, Dong M, Yu W. An emergency aircraft evacuation simulation considering passenger overtaking and luggage retrieval. Reliab Eng Syst Saf 2022:108851.
[24] Fu Z, Xia L, Yang H, Liu X, Ma J, Luo L, Yang L, Chen J. Simulation study of overtaking in pedestrian flow using floor field cellular automaton model. Int J Mod Phys C 2017;28.
[25] von Schantz A, Ehtamo H. Pushing and overtaking others in a spatial game of exit congestion. Phys A: Stat Mech Appl 2019;527:121151.
[26] Peng J, Wei Z, Chen Y, Wang S, Li Y, Chen L, Taku F. A micro-action-based decision-making framework for simulating overtaking behaviors of heterogeneous pedestrians. Inf Fusion 2025;117:102898.
[27] Xu C, Witlox F. Understanding total evacuation time perception in airplane emergency: a stated preference approach. Saf Sci 2022;146:105540.
[28] Helbing D, Farkas I, Vicsek T. Simulating dynamical features of escape panic. Nature 2000;407:487–90.
[29] Hedo J, Martinez-Val R. Computer model for numerical simulation of emergency evacuation of transport aeroplanes. Aeronaut. J 2010;114:737–46.
[30] Burstedde C, Klauck K, Schadschneider A, Zittartz J. Simulation of pedestrian dynamics using a two-dimensional cellular automaton. Phys A: Stat Mech Appl 2001;295:507–25.
[31] Guo C, Huo F, Li Y, Li C, Zhang J. An evacuation model considering pedestrian crowding and stampede under terrorist attacks. Reliab Eng Syst Saf 2024:110230.
[32] Li Y, Yang X, Wang Z, Chen L, Chen Y. Lane-design for mixed pedestrian flow in T-shaped passage. Phys A: Stat Mech Appl 2022;589:126593.
[33] Huang R, Zhao X, Zhou C, Kong L, Liu C, Yu Q. Static floor field construction and fine discrete cellular automaton model: algorithms, simulations and insights. Phys A: Stat Mech Appl 2022;606:128150.
[34] Lv W, Song Y, Wang Z, Fang Z. Analysis of evacuation risk for passengers in large single-decker city bus. China Saf Sci J 2014;24.
[35] Liang J, Zhang Y-f, Huang H. The experiment and simulation analysis of bus emergency evacuation. Procedia Eng 2018;211:427–32.
[36] Xu H-H, Guo R-Y. Emergency passenger evacuation from bus carriage: Results from realistic data and modeling simulations. J Manag Sci Eng 2022.
[37] Galea E, Blackshields D, Finney K, Cooney D. Passenger train emergency systems: development of prototype railEXODUS software for US passenger rail car egress. In: United States. Federal Railroad Administration. Office of Research and Development; 2014.
[38] Qiu H, Fang W. Effect of high-speed train interior space on passenger evacuation using simulation methods. Phys A: Stat Mech Appl 2019;528:121322.
[39] Najmanová H, Kuklík L, Pešková V, Bukáček M, Hrabák P, Vašata D. Evacuation trials from a double-deck electric train unit: experimental data and sensitivity analysis. Saf Sci 2022;146:105523.
[40] Liu Y, Wang W, Huang H-Z, Li Y, Yang Y. A new simulation model for assessing aircraft emergency evacuation considering passenger physical characteristics. Reliab Eng Syst Saf 2014;121:187–97.
[41] Melis DJ, Silva JM, Yeun R, Wild G. The effect of airline passenger anthropometry on aircraft emergency evacuations. Saf Sci 2020;128:104749.
[42] Wang X, Liu Z, Loughney S, Yang Z, Wang Y, Wang J. Numerical analysis and staircase layout optimisation for a Ro-Ro passenger ship during emergency evacuation. Reliab Eng Syst Saf 2022;217:108056.
[43] Xie Q, Guo S, Zhang Y, Wang C, Ma C, Li Q. An integrated method for assessing passenger evacuation performance in ship fires. Ocean Eng 2022;262:112256.
[44] Xie C, Huang L, Wang R, Deng J, Shu Y. Ship fire modelling and evacuation simulation in navigation tunnel. Tunn Undergr Space Technol 2022;126:104546.
[45] Fang S, Liu Z, Wang X, Wang J, Yang Z. Simulation of evacuation in an inclined passenger vessel based on an improved social force model. Saf Sci 2022;148:105675.
[46] Chen M, Guo M, Han D, Yuan L, Li Y, Wu K. A pedestrian evacuation model for a ship's flat multi-exit large space under fire environment. Ocean Eng 2024;309:118570.
[47] K. Miyazaki, H. Matsukura, M. Katuhara, K. Yoshida, S. Ota, N. Kiriya, O. Miyata, Behaviors of pedestrian group overtaking wheelchair user, National Maritime Research Institute (NMRI)(Report 181-0004). Shinkawa Mitakashi, Tokyo, Japan, (2004).

[48] Ji X, Zhou X, Ran B. A cell-based study on pedestrian acceleration and overtaking in a transfer station corridor. Phys A: Stat Mech Appl 2013;392:1828–39.
[49] General Administration of Quality Supervision. Inspection and quarantine of the P. R. China, human dimensions of Chinese adults. Beijing: Standards Press of China; 1988.
[50] Bender R, Augustin T, Blettner M. Generating survival times to simulate Cox proportional hazards models. Stat Med 2005;24:1713–23.
[51] Zhang S, Huang R, Yu Q. An experimental study on evacuation characteristics and restrictive factors for passengers evacuating from a motorcoach. China Saf Sci J 2019;29:181–7.
[52] von Sivers I, Köster G. Dynamic stride length adaptation according to utility and personal space. Transp Res B: Methodol 2015;74:104–17.
[53] Weidmann U. Transporttechnik der fußgänger: transporttechnische eigenschaften des fußgängerverkehrs, literaturauswertung. IVT Schriftenr 1993;90.
[54] Samson MM, Crowe A, de Vreede PL, Dessens JAG, Duursma SA, Verhaar HJJ. Differences in gait parameters at a preferred walking speed in healthy subjects due to age, height and body weight. Aging Clin Exp Res 2001;13:16–21.
[55] Yanagisawa D, Kimura A, Tomoeda A, Nishi R, Suma Y, Ohtsuka K, Nishinari K. Introduction of frictional and turning function for pedestrian outflow with an obstacle. Phys Rev Stat Nonlin Soft Matter Phys 2009;80:036110.
[56] Ronchi E, Reneke PA, Peacock RD. A method for the analysis of behavioural uncertainty in evacuation modelling. Fire Technol 2014;50:1545–71.
[57] Galea E, Deere S, Filippidis L, Brown R, Nicholls I, Hifi Y, Besnard N. The SAFEGUARD validation data-set and recommendations to IMO to update MSC Circ 1238. In: SAFEGUARD passenger evacuation seminar, the royal institute of naval architects; 2012.